12 Nuclear Astrophysics

12.1 Introduction

The hydrogen, deuterium, and most of the helium atoms in the universe are believed to have been created some 20 billion years ago in a primary formation process referred to as the Big Bang, while all other elements have been formed—and are still being formed—in nuclear reactions in the stars. These reaction processes can only be understood in an astrophysical context, as briefly outlined in this chapter, which also describes how nuclear science has provided much understanding about the universe, our solar system and our planets.

The evolution of the universe is the object of study of cosmology and astrophysics; nuclear astrophysics studies the synthesis of heavy nuclei starting from lighter ones in temperature and pressure conditions existing in the stars. Nuclear physics studies the behavior of nuclei under normal conditions or in excited states, as well as the reactions among them. Chemistry studies the structure of the atomic molecules and the reactions among them. Finally, biology studies the formation and development of great molecular agglomerates that compose living beings. In any of these sciences the objective is to understand complex structures starting from simpler structures and from the interactions among them.

Nuclear astrophysics is the field concerning "the synthesis and evolution of atomic nuclei, by thermonuclear reactions, from the Big Bang to the present. What is the origin of the matter of which we are made?" Our high entropy universe, presumably resulting from the Big Bang, contains many more photons than particles of matter with mass, for example, electrons, protons, and neutrons. Because of the high entropy and the consequent low density of matter (on terrestrial or stellar scales) at any given temperature as the universe expanded, there was time to manufacture elements only up to helium, and the major products of cosmic nucleosynthesis remained hydrogen and helium. Stars formed from this primordial matter and used these elements as fuel to generate energy like a giant nuclear reactor. In the process, the stars could shine and manufacture the higher

atomic number elements like carbon, oxygen, calcium, and iron of which we and our world are made. The heavy elements are either dredged up from the core to the surface of the star, from which they are dispersed by stellar wind or directly ejected into the interstellar medium when a (massive) star explodes. This stardust is the source of heavy elements for new generations of stars and sunlike systems.

The sun is slowly burning a light element, hydrogen, into a heavier element, helium. It is not exactly the same now as when it first started burning hydrogen in its core and will start to look noticeably different once it exhausts all the core hydrogen. In other words, nuclear reactions in the interiors of stars determine the evolution or the life cycle of the stars, apart from providing them with internal power for heat and light and manufacturing all the heavier elements that the early universe could not.

The emphasis here is on the nuclear reactions in stars and how these are calculated, rather than how stars evolve. The latter usually forms a core area of stellar astrophysics. There is a correspondence between the evolutionary state of a star, its external appearance and internal core conditions, and the nuclear fuel it burns—a sort of a mapping between the astronomer's Hertzsprung-Russell diagram and the nuclear physicist's chart of the nuclides, until nuclear burning takes place on too rapid a timescale.

12.2 Astronomical Observations

12.2.1 *The Milky Way*

The stars we directly can see all belong to our galaxy, the Milky Way, which is a spiral galaxy, about 30 kpc across and 1 kpc thick. (The kpc, kiloparsec, is the common astronomical unit of distance; 1 parsec is 3.1×10^{16} m, or 3.26 light years, ly.) Thus light travels across our galaxy in about 100,000 years. The Milky Way contains some 200×10^9 stars, and interstellar dust and gas (~200 pc thick) that spreads out to a diameter of about 50 kpc (hot gas atoms, the *halo*). Our sun is located at the outer edge of one of the spiral arms, about 8.5 kpc from the galactic center. The dust limits sight toward the center to only a few kpc; without this dust the galactic center would shine as bright as our sun. The stars in our galaxy move tangentially around its center with angular velocities increasing closer to the center, indicating the existence of a heavy central object, called Sagittarius (Sgr) A*.

The Milky Way belongs to the Local Group, a cluster of some 20 galaxies that include the Large Magellanic Cloud, our nearest galaxy, 50 kpc away, and the Andromeda galaxy, 650 kpc away. The Local Group is part of the larger Virgo supercluster. The universe contains some 10^{10} galaxies. The galaxies fill only a fraction of space, less than 5%, the rest appears void of matter.

In the 1930s Hubble discovered that galaxies on the whole are equally distributed in all directions of space as observed from the earth. Thus space—on a large scale—seems to be isotropic. This idea of uniformity of the universe is called the *cosmological principle*. This information has been deduced from celestial mechanics (motion of bodies according to Newton's fundamental laws) and from spectroscopic analysis of light and other kinds of

radiation. It has been found that the mass of our sun is 1.99×10^{30} kg (=1 solar mass, $M_\odot$). The mass of the Milky Way is $>2 \times 10^{11}\ M_\odot$; about 10% of the mass is interstellar gas, and 0.1% is dust (typically particles with diameter 0.01–0.1 μm). The interstellar gas density varies considerably in our galaxy; in our part of space it varies from about 10^9 (in dark clouds) to 10^5 atoms/m^3 (on the average $\sim$1 atom/cm^3). Though it contains mainly H and He, large rather complex molecules containing H, C (up to C_{15} molecules), N, and O (including amino acids) have also been discovered.

12.2.2 *Dark matter*

Astronomical models of the universe indicate that it will expand forever if the observed galaxies alone account for the total mass of the universe. Almost 90% is missing of the mass needed for a slowing down and ultimately contracting universe. Most cosmologists believe that the mass of the observed galaxies is less than 10% of the mass of the universe, the main part consisting of *dark matter*; this includes interstellar and intergalactic matter, neutron stars, "black holes," and other little-known sources of radiation, like quasars, whose masses are unknown.

From mechanics and Newton's gravitational law one can calculate the velocity needed for a body, m_x, to escape the gravitational pull of a larger mass, m, where $m_x \ll m$. For example, if m is the earth's mass (5.94×10^{24} kg), a rocket (mass m_x) must have a velocity of about 11 km/s to escape from the earth's surface (the escape velocity, v_e). Conversely, for a given velocity, v_e, one can calculate the mass and size of the large body needed to hamper such an escape. A body with our solar mass, $M_\odot$, but a radius of only 3 km, requires an escape velocity $>3 \times 10^{10}$ m/s. Thus not even light will escape such a body, which therefore is termed a *black hole*. Though we cannot observe black holes directly, some secondary effects can be observed.

Astronomical observations of star movements support the existence of black holes. For example, from movements of stars close to our galactic center, it is believed that a black hole is located at SgrA* in the center of the Milky Way, with a mass $>3 \times 10^6\ M_\odot$. The radius of such a hole would be the same as that of our sun. The density of matter in the hole would be several million times that of our sun (the average value for the sun is about 1400 kg/m^3). Obviously matter cannot be in the same atomic state (nuclei surrounded by electrons) as we know on earth. Instead, we must assume that the electron shells are partly crushed; we refer to this as *degenerate matter*, because the electron quantum rules cannot be upheld. For completely crushed atoms, matter will mainly consist of compact nuclei. For example, for calcium the nuclear density is $\sim 2.5 \times 10^{17}$ kg/m^3.

Even if black holes are given a considerable portion of the missing mass, this will not be enough. However, a very recent discovery may provide the "missing" mass: detailed analysis of the variation in luminosity (a factor of about 2.5) for some 10 million double stars in the Large Magellanic Cloud gives support for the existence of nearby *gravitational microlenses*, which are believed to be unborn stars (so-called *brown dwarfs*) of sizes $\sim 10\ M_\odot$. When such a dark object passes the line of sight to a distant star it acts as a focusing lens for the light, thereby temporarily increasing that star's apparent luminosity. As these

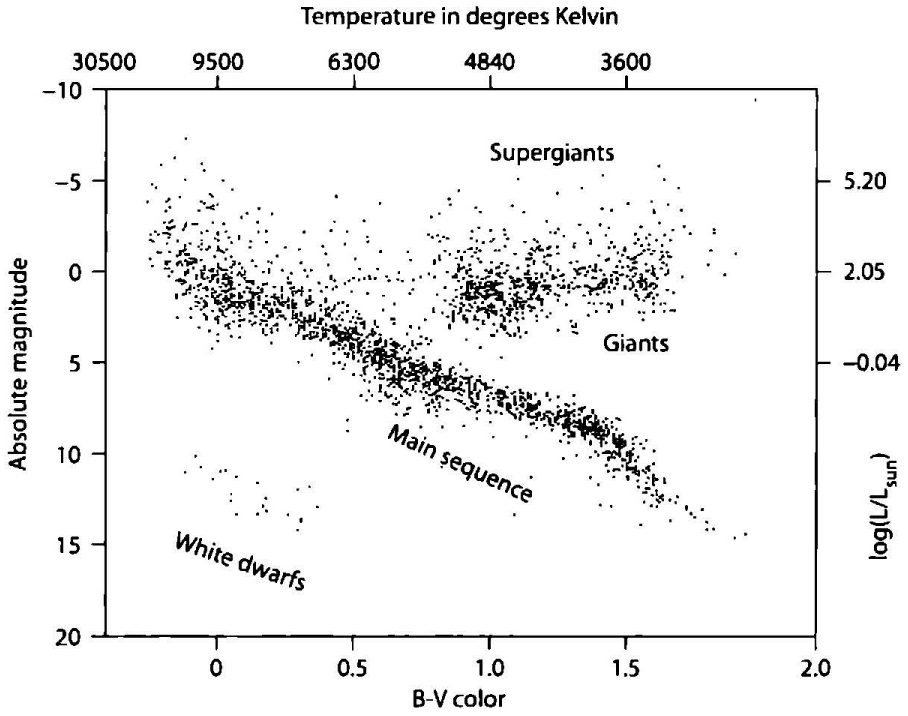

Figure 12.1 *HR* diagram showing surface temperature, spectral class, and color for stars born on the main sequence as a function of their absolute luminosity relative to the solar mass $M_{\odot}$.

gravitational microlenses seem to be especially abundant in the halo of our galaxy (and presumably in halos of other galaxies), they—together with neutron stars and black holes—could account for the 90% of "missing dark matter" required for an ultimately contracting universe.

12.2.3 Luminosity and Hubble's law

Spectral analysis of the light received from astronomical objects has provided us with information about their (surface) temperature (from their continuous spectrum) and outer chemical composition (from identification of spectral line frequencies), while bolometric measurements have given their luminosity (energy flux density, F/Wm^2). In 1911 Hertzsprung and Russell discovered that, if the luminosity and color (or temperature) of stars in different galaxies is compared with those of similar types of stars in the Milky Way, the stars are distributed according to a certain pattern, the so-called Zero Age Main Sequence (ZAMS); it is believed that most stars in their evolution follow the diagram beginning at the lower right side, along the main sequence into the red giant phase, then to the left and down, decreasing in size and temperature to end as blue or white dwarfs.

Hertzsprung-Russell (HR) diagrams, like the one in figure 12.1, are valid for stars of about 0.7–70 $M_{\odot}$: from such diagrams conclusions can be drawn about the size (or mass) and relative age of the star, as it is assumed that stars of a given mass follow the same sequence as they age. The apparent luminosity, F, which we observe with our telescopes, is related to

the *absolute luminosity*, L^*, the total energy flux in all directions from a star, by the relation

$$F = \frac{L^*}{4Bd^2}, \tag{12.1}$$

where d is the distance from the star. The historical classification of stars into brightness classes is now usually replaced by their relative (or apparent) magnitude, m^*, defined as $m = -2.5 \log (F/F_0)$, where F_0 is a reference flux density.

Hubble discovered that all galaxies, except for those in Virgo, show a spectral red shift (increased distance between known frequency lines). This is assumed to be a Doppler effect due to the objects moving away from us (compare the lowering of the pitch from the horn of a train moving away from us). The red shift z is

$$z = (\lambda - \lambda_0)/\lambda_0 = Hd/c\,, \tag{12.2}$$

where H is the *Hubble constant*. For velocities $v \ll c$, the relation becomes $z = v/c$, hence

$$v_r = Hd\,, \tag{12.3}$$

which is the common expression of *Hubble's law*; v_r is the radial velocity. If the red shift is plotted against the apparent magnitude of the brightest star in a large number of galaxies, it is seen to increase with decreasing luminosity, which is interpreted as that the more distant (faintest) galaxies move away from us faster than the closer ones. Except for the galaxies in the Local Group, all galaxies recede from us with velocities up to 20,000 km/s; hence it is concluded that the universe is expanding.

If the universe is expanding, the galaxies were once much closer to each other. If the rate of expansion has been unchanged, the inverse of the Hubble constant, H^{-1}, would represent the age of the universe. In (12.3) v_r is the radial velocity of a galaxy at distance d from us. But velocity is just distance divided by time; that is, $v_r = d/t_0$, where t_0 is the time the expansion has going on, assuming a constant speed. Thus, $d/t_0 = Hd$, or $t_0 = 1/H$. t_0 is only an upper limit of the age of the universe, because we have reasons to believe that the expansion has slowed down due to gravitational pull. According to present estimates an Hvalue of 0.05–0.1 $\mathrm{ms}^{-1}\ \mathrm{pc}^{-1}$ corresponds to an age of 10–20 Gy (gigayears, 10^9 years). Cosmologists also give the age in "scale factor" $(1 + z)$-values (red shift values); for example, we would observe a z-value of 10 for an object about one billion years old from the formation of the universe.

12.3 The Big Bang

In 1965 it was discovered that low energy microwave radiation (at 7.35 cm uncorrected) reaches us from all directions in space (about 400 photons cm^{-3}). This is referred to as the cosmic background radiation, whose wavelength corresponds to radiation from a black body of temperature 2.7 K (about 0.0003 eV). Thermodynamic calculations show that this is the temperature reached after adiabatic expansion of a very hot cloud for some 10 billion

years. The existence of such background radiation was predicted by Gamow decades before in a cosmological hypothesis referred to as the *Big Bang model*.

The Big Bang hypothesis requires an instantaneous beginning of our universe at a point at which all energy is concentrated. Ordinary nuclear reactions cannot model this beginning, and we must turn to particle physics.

In the following we describe the formation of the universe and the elements according to the so-called *standard model of stellar evolution*, based on the models originally developed by Bethe and Weizsaecker in the 1930s for the reactions in the sun, and the Big Bang hypothesis for the formation of the universe as originally suggested in 1948 by Gamow, Alpher, and Herman, and later developed by the B^2FH group, Weinberg, and others.

Around "time zero," the universe consisted of an immensely dense, hot sphere of photons, quarks, leptons, and their antiparticles, in thermal equilibrium, particles being created by photons and photons by annihilation of particles. The temperature must have been $\geq 10^{13}$ K, but no light was emitted, because the enormous gravitational force pulled the photons back. The system was supposed to be in a unique state with no repulsion forces. However, just as a bottle of supercritical (overheated) water can explode by a phase transition, so did the universe, and time began. The universe expanded violently in all directions, and as age and size grew, density and temperature fell.

One-hundredth of a second later all the quarks were gone, and the universe consisted of an approximately equal number of electrons, positrons, neutrinos, and photons, with a small number of protons and neutrons; the ratio of protons to photons is assumed to have been about 10^{-9}. The temperature was about 10^{11} K and the density so high, about 4×10^6 kg m^{-3}, that even the unreactive neutrinos were hindered in escaping. The conditions can be partly understood by considering the relations

$$E(MeV) = mc^2 = 931.5\Delta M, \tag{12.4}$$

which gives the energy required to create a particle of mass ΔM (E in MeV, ΔM in atomic mass units, u), and

$$E(MeV) = kT = 8.61 \times 10^{-11}\ T, \tag{12.5}$$

which gives the average kinetic energy of a particle at temperature T (K, Kelvin).

As the photon energy of E (eV) corresponds to the wavelength λ (m) according to

$$E(eV) = h\nu = hc/\lambda = 1.240 \times 10^{-6}/\lambda(\text{m}), \tag{12.6}$$

one can estimate that the creation of a proton or a neutron (rest mass 940 MeV) from radiation requires a temperature of 1.1×10^{13} K, corresponding to a photon wave length of about 10^{-15} m, the size of a nucleon. At these temperatures nucleons are formed out of radiation, but are also disrupted by photons, leading to an equilibrium with about an equal number of protons and neutrons. At temperatures below the threshold formation energy, no nucleons are formed. However, it should be remembered that particles and radiation are distributed over a range of energies, according to the Boltzmann and Planck distribution laws. Thus some formation (and disruption) of nucleons occurs even at lower temperatures.

In about 0.1 s the temperature is assumed to have decreased to 3×10^{10} K (corresponding to 2.6 MeV). Now, the equilibrium between protons, neutrons, electrons, and neutrinos can be written

$$p + \bar{\nu} = n + e^+ \ (Q = -1.80\,\text{MeV}) \quad \text{and} \quad n + \nu = p + e^- \ (Q = 0.78\,\text{MeV}) . \tag{12.7}$$

The mass of the neutron exceeds that of the proton by a small margin of 0.00013885 u, corresponding to 1.29 MeV; thus reaction on the left of (12.7) requires energy, while reaction on the right releases energy. The formation of protons was therefore favored over that of neutrons, leading to 38% neutrons and 62% protons.

As temperature and density further decreased, the neutrinos began to behave like free particles, and below 10^{10} K they ceased to play any active role in the formation sequence (matter became transparent to the neutrinos). The temperature corresponded then to ~1 MeV, about the threshold energy for formation of positron/electron pairs. Consequently they began to annihilate each other, leaving, for some reason, a small excess of electrons. Though neutrons and protons may react at this temperature, the thermal energies were still high enough to destroy any heavier nuclides eventually formed.

After 14 s the temperature had decreased to 3×10^9 K (0.27 MeV), and 3 min later it had reached about 10^9 K (<0.1 MeV). Now, with the number of electrons, protons, and neutrons about equal (though the universe mostly consisted of photons and neutrinos), some protons and neutrons reacted to form stable nuclides like deuterium and helium. However, for the deuteron to be stable, the temperature must decrease below the Q-value for its formation, about 10^{10} K, and, in reality, to the much lower value of about 10^9 K, because of the high photon flux, which may dissociate the deuteron into two protons. Two deuterium atoms then fuse, probably in several steps as discussed below, to form He. He is an extremely stable nucleus, not easily destroyed, as compared to nuclides with masses >4, whose binding energies (per nucleon) are only a few MeV (figure 4.3).

As the universe expanded, the probability for particle collisions decreased, while the kinetic energy available for fusion reactions was reduced. Therefore, nucleon build-up in practice stopped with ^{4}He, leading to an average universal composition of 73% hydrogen and 27% helium. A very small amount of deuterium was still left, as well as a minute fraction of heavier atoms, formed by the effects of the "Boltzmann tail" and "quantum tunneling." The remaining free neutrons (half-life 10.4 min) now decayed to protons. The situation about 35 minutes after time zero was then the following: temperature 3×10^8 K, density about 10^{-4} kg m^{-3}. The universe consisted of 69% photons, 31% neutrinos, and a fraction of 10^{-9} of particles consisting of 72–78% hydrogen, 28–22% helium, and an equivalent number of free electrons, all rapidly expanding in all directions of space.

It was still too hot for the electrons to join the hydrogen and helium ions to form neutral atoms. This did not occur until about 500,000 years later, when the temperature had dropped to a few 1,000 K. The disappearance of free electrons broke the thermal contact between radiation and matter, and radiation continued to expand freely. An outside spectator would have observed this as a huge flash and a rapidly expanding fireball. In the adiabatic expansion the radiation cooled further to the cosmic background radiation level of

2.7 K measured today. The recent observation that the cosmic background radiation shows ripples in intensity in various directions of space indicates a slightly uneven ejection of matter into space, allowing gravitational forces to act, condensing the denser cloud parts into even more dense regions, or "islands," which with time separated from each other, leaving seemingly empty space in between. Within these clouds, or proto-galaxies, local higher densities led to the formation of stars.

12.4 Stellar Evolution

12.4.1 *Stars burn slowly*

Energy production in the stars is a well-known process. The initial energy that ignites the process arises from the gravitational contraction of a mass of gas. The contraction increases the pressure, temperature, and density at the center of the star until values are achieved that are able to start thermonuclear reactions, initiating the star lifetime. The energy liberated in these reactions yields a pressure in the plasma, which opposes compression due to gravitation. Thus, an equilibrium is reached for the energy produced, the energy liberated by radiation, temperature, and pressure.

The sun is a star in its initial phase of evolution. The temperature at its surface is 6000° C, while in the interior it reaches 1.5×10^7 K, with a pressure of 6×10^{11} atm and density 150 g/cm^3. The present mass of the sun is $M_\odot = 2 \times 10^{33}$ g and its main composition is hydrogen (70%), helium (29%), and less than 1% heavier elements, like carbon, and oxygen.

For reactions involving charged particles, nuclear physicists often encounter cross sections near the Coulomb barrier of the order of millibarns. One can obtain a characteristic luminosity L_C based on this cross section and the nuclear energy released per reaction [Bah89]:

$$L_C \sim \epsilon N \Delta E / \tau_C, \tag{12.8}$$

where $\epsilon \approx 10^{-2}$ is the fraction of the total number of solar nuclei $N \sim 10^{57}$ that take part in nuclear fusion reactions, generating typically $\Delta E \sim 25$ MeV in hydrogen to helium conversion. Here, the τ_C is the characteristic timescale for reactions, which becomes minuscule for the cross sections at the Coulomb barrier, the ambient density and relative speed of the reactants, and so on:

$$\tau_C \sim \frac{1}{n\sigma v} = \frac{10^{-8}\text{s}}{|n/(10^{26}\text{cm}^{-3})||\sigma/mb||v/10^9\text{cm s}^{-1}|}. \tag{12.9}$$

This would imply a characteristic luminosity of $L_C \approx 10^{20} L_\odot$, even for a small fraction of the solar material taking part in the reactions ($\epsilon \sim 10^{-2}$). If this were really the appropriate cross section for the reaction, the sun would have been gone very quickly indeed. Instead, the cross sections are much less than that at the Coulomb barrier penetration energy (say, at proton energies of 1 MeV), to allow for a long lifetime of the sun (in addition the weak interaction process gives a smaller cross section for some reactions than the electromagnetic process.

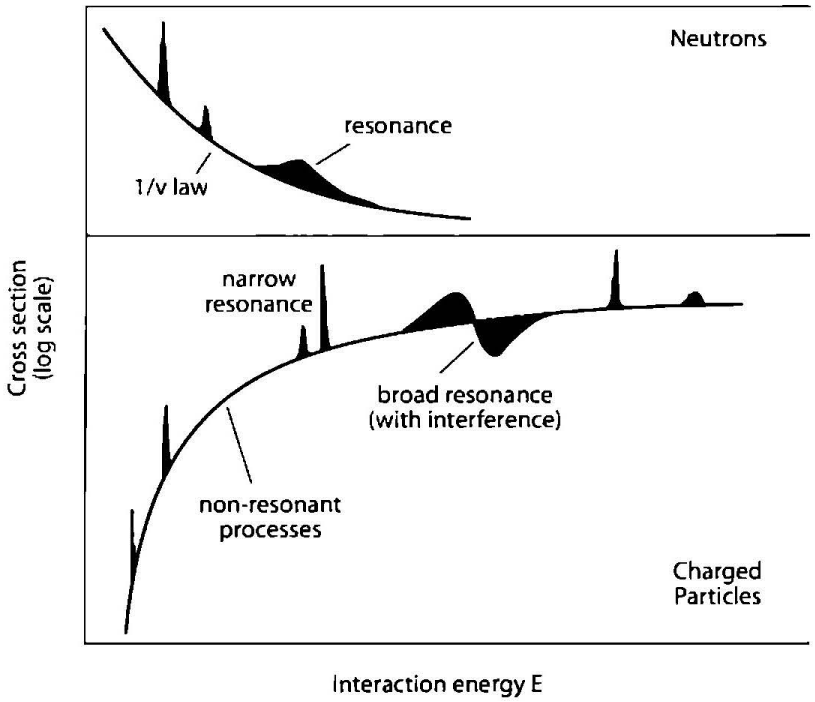

Figure 12.2 Dependence of total cross sections on the interaction energy for neutrons (top panel) and charged particles (bottom panel). Note the presence of resonances (narrow or broad) superimposed on a slowly varying nonresonant cross section.

Stellar nuclear reactions can be either charged particle reactions (both target and projectile are nuclei) or neutral particle (neutron)-induced reactions. Both reactions can go through a resonant state of an intermediate nucleus or can be nonresonant. In the former case, the intermediate state can be a narrow unstable state, which decays into other particles or nuclei. In general, a given reaction can involve both types of reaction channels. In charged particle-induced reactions, the cross section for both reaction mechanisms drops rapidly with decreasing energy, due to the effect of the Coulomb barrier (and thus it becomes more difficult to measure stellar reaction cross sections accurately). In contrast, the neutron induced reaction cross-section is very large and increases with decreasing energy (here, resonances may be superposed on a smooth nonresonant yield which follows the $1/v \sim 1/\sqrt{E}$ dependence). These reaction rates and cross sections can be then directly measured at stellar energies that are relevant (if such nuclei are long lived or can be generated). The schematic dependence of the cross sections is shown in figure 12.2.

12.4.2 *Gamow peak and astrophysical S-factor*

The sun and other "main sequence" stars (burning hydrogen in their core quiescently) evolve very slowly by adjusting their central temperature such that the average thermal energy of a nucleus is small compared to the Coulomb repulsion an ion-ion pair encounters. This is how stars can live for astronomically long times. A central temperature $T \geq 10^7$K (or $T_7 \geq 1$; hereafter a subscript x to temperature or density indicates a temper-

ature in units of 10^x) is required for sufficient kinetic energy of the reactants to overcome the Coulomb barrier and for thermonuclear reactions involving hydrogen to proceed at an effective rate, even though fusion reactions have positive Q-values, that is, net energy is liberated out of the reactions.

The classical turning point radius for a projectile of charge Z_2 and kinetic energy E_p (in a Coulomb potential $V_C = Z_1 Z_2 e^2/r$, and an effective height of the Coulomb barrier $E_C = Z_1 Z_2 e^2/R_n = 550$ keV for a p + p reaction), is $r_{cl} = Z_1 Z_2 e^2/E_p$. Thus, classically a p + p reaction would proceed only when the kinetic energy exceeds 550 keV. Since the number of particles traveling at a given speed is given by the *Maxwell-Boltzmann* (MB) distribution $\phi(E)$, only the tail of the MB distribution above 550 keV is effective when the typical thermal energy is 0.86 keV ($T_9 = 0.01$). The ratio of the tails of the MB distributions: $\phi(550\text{ keV})/\phi(0.86\text{ keV})$ is quite minuscule, and thus classically at typical stellar temperatures this reaction will be virtually absent.

Although classically a particle with projectile energy E_p cannot penetrate beyond the classical turning point, quantum mechanically, one has a finite value of the square wave function at the nuclear radius R_n : $|\psi(R_n)|^2$. The probability that the incoming particle penetrates the barrier is

$$P = \frac{|\psi(R_n)|^2}{|\psi(R_c)|^2}, \tag{12.10}$$

where $\psi(r)$ are the wavefunctions at corresponding points.

Bethe [Bet37] solved the Schröedinger equation for the Coulomb potential and obtained the transmission probability

$$P = \exp\left(-2KR_c\left[\frac{\tan^{-1}(R_c/R_n - 1)^{1/2}}{(R_c/R_n - 1)^{1/2}} - \frac{R_n}{R_c}\right]\right). \tag{12.11}$$

with $K = |2\mu/\hbar^2(E_c - E)|^{1/2}$. This probability reduces to a much simpler relation at the low energy limit $E \ll E_c$, which is equivalent to the classical turning point R_c being much larger than the nuclear radius R_n. The probability is

$$P = \exp(-2\pi\eta) = \exp\left[-2\pi Z_1 Z_2 e^2/(\hbar v)\right] = \exp\left[-31.3 Z_1 Z_2 \left(\frac{\mu}{E}\right)^{1/2}\right], \tag{12.12}$$

where in the second equality μ is the reduced mass in u and E is the center of mass energy in keV.

The exponential quantity involving the square brackets in the second expression is called the *Gamow factor*. The reaction cross section between particles of charge Z_1 and Z_2 has this exponential dependence due to the Gamow factor. In addition, because the cross sections are essentially "areas" proportional to $\pi(\lambda/2\pi\hbar)^2 \propto 1/E$, it is customary to write the cross section with these two energy dependencies filtered out,

$$\sigma(E) = \frac{\exp(-2\pi\eta)}{E} S(E), \tag{12.13}$$

where the factor is called the astrophysical (or nuclear) S-factor.

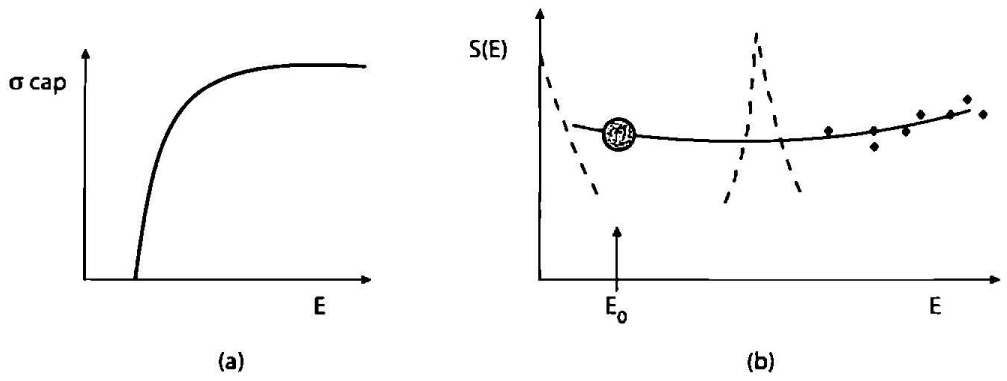

Figure 12.3 Cross section and astrophysical S-factor for charged particle reactions as a function of beam energy. The effective range of energy in stellar interiors is usually far less than the Coulomb barrier energy E_C or the lower limit E_L, where laboratory measurements can be carried out. The cross section drops sharply in the region of astrophysical interest, whereas the change is much less severe for the S-factor. Therefore, necessary extrapolation of laboratory data to lower energies relevant for astrophysical situations is more reliable in the case of the S-factor.

The S-factor may contain degeneracy factors due to spin, for example, $[(2J+1)/(2J_1+1)(2J_2+1)]$, as reaction cross sections are summed over final states and averaged over initial states. Because the rapidly varying parts of the cross section (with energy) are thus filtered out, the S-factor is a slowly varying function of center of mass energy, at least for the nonresonant reactions. It is thus much safer to extrapolate $S(E)$ to the energies relevant for astrophysical environments from the laboratory data, which are usually generated at higher energies (due to difficulties of measuring small cross sections), than directly to extrapolate the $\sigma(E)$, which contains the Gamow transmission factor (see figure 12.3). Additionally, in order to relate $\sigma(E)$ and $S(E)$, quantities measured in the laboratory to these relevant quantities in the solar interior, a correction factor f_0 due to the effects of electron screening needs to be taken into account [Sal54].

In the stellar core with a temperature T, reacting particles have many different velocities (energies) according to a Maxwell-Boltzmann distribution

$$\phi(v) = 4\pi v^2 \left(\frac{\mu}{2\pi kT}\right)^{3/2} \exp\left[-\frac{\mu v^2}{2kT}\right] \propto E \exp(-E/kT). \tag{12.14}$$

Nuclear cross sections or the reaction rates which also depend upon the relative velocity (or equivalently the center of mass energy) therefore need to be averaged over the thermal velocity (energy) distribution. Therefore, the thermally averaged reaction rate per particle pair is

$$\langle \sigma v \rangle = \int_0^\infty \phi(v)\sigma(v)v\,dv = \left(\frac{8}{\pi\mu}\right)^{1/2} \frac{1}{(kT)^{3/2}} \int_0^\infty \sigma(E)E \exp(-E/kT)dE. \tag{12.15}$$

The thermally averaged reaction rate per pair is, utilizing the astrophysical S-factor and the energy dependence of the Gamow factor,

$$\langle \sigma v \rangle = \left(\frac{8}{\pi\mu}\right)^{1/2} \frac{1}{(kT)^{3/2}} \int_0^\infty S(E) \exp\left[-\frac{E}{kT} - \frac{b}{\sqrt{E}}\right] dE, \tag{12.16}$$

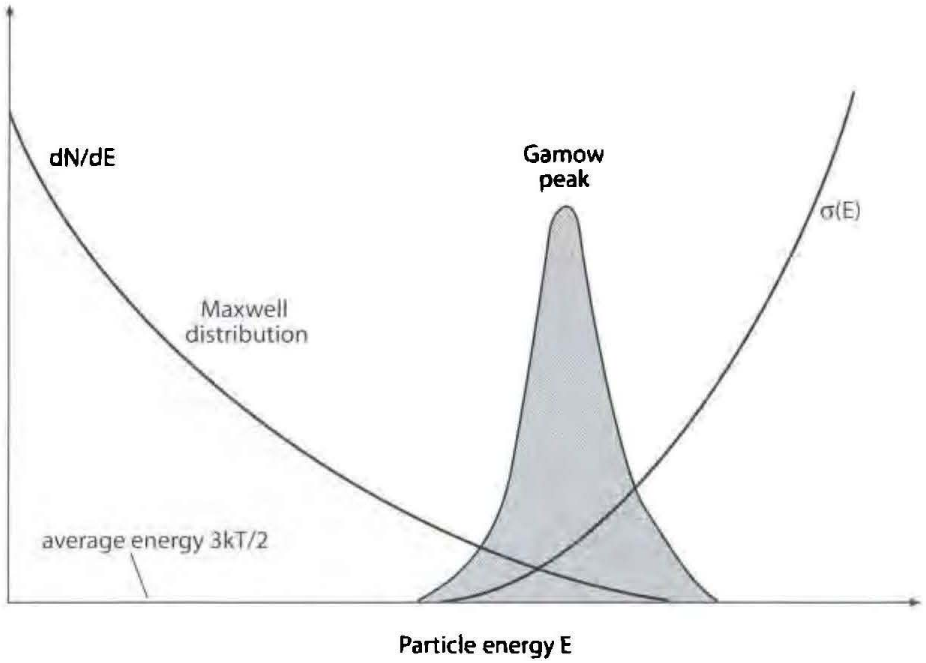

Figure 12.4 The Gamow peak is a convolution of the energy distribution of the Maxwell-Boltzmann probability and the quantum mechanical Coulomb barrier transmission probability. The peak in the shaded region near energy E_0 is the Gamow peak that gives the highest probability for charged particle reactions to take place. Usually the Gamow peak is at a much higher energy than kT, and in the figure the ordinate scale (for the Gamow peak) is magnified with respect to those of the Maxwell-Boltzmann and barrier penetration factors.

with $b^2 = E_G = 2\mu(\pi e^2 Z_1 Z_2/\hbar)^2 = 0.978\mu Z_1^2 Z_2^2$ MeV, E_G being called the Gamow energy. Note that in the expression for the reaction rate above, at low energies, the exponential term $\exp(-b/\sqrt{E}) = \exp(-\sqrt{(E_G/E)})$ becomes very small, whereas at high energies the Maxwell-Boltzmann factor $\exp(-E/kT)$ vanishes. Hence there would be a peak (at energy, say, E_0) of the integrand for the thermally averaged reaction rate per pair (see figure 12.4).

The exponential part of the energy integrand can be approximated as

$$\exp\left[-\frac{E}{kT} - bE^{-1/2}\right] \sim C\exp\left[-\left(\frac{E-E_0}{\Delta/2}\right)^2\right], \tag{12.17}$$

where

$$C = \exp(-E_0/kT - bE_0^{-1/2}) = \exp(-3E_0/kT) = \exp(-\tau), \tag{12.18}$$

with

$$E_0 = (bkT/2)^{\frac{2}{3}} = 1.22\text{keV}(Z_1^2 Z_2^2 \mu T_6^2)^{\frac{1}{3}}, \tag{12.19}$$

and $\text{Delta} = 0.75\text{keV}(Z_1^2 Z_2^2 A T_6^5)^{1/6}$

(12.20)

Table 12.1 Parameters of the thermally averaged reaction rates at $T_6 = 15$.

Reaction	Coulomb barrier (MeV)	Gamow peak (E_0) (keV)	I_{max} ($e^{-3E_0/kT}$)	Δ (keV)	$(\Delta)I_{max}$
p + p	0.55	5.9	1.1×10^{-6}	6.4	7×10^{-6}
p + N	2.27	26.5	1.8×10^{-27}	13.6	2.5×10^{-26}
$\alpha + C^{12}$	3.43	56	3×10^{-57}	19.4	5.9×10^{-56}
$O^{16} + O^{16}$	14.07	237	6.2×10^{-239}	40.4	2.5×10^{-237}

Since most stellar reactions happen in a fairly narrow band of energies, $S(E)$ will have a nearly constant value over this band averaging to S_0. With this, the reaction rate per pair of particles turns out to be

$$\langle \sigma v \rangle = \left[\frac{8}{\pi\mu(kT)^3}\right]^{1/2} S_0 \int_0^\infty \exp\left(-\tau - 4\left(\frac{E-E_0}{\Delta}\right)^2\right) dE$$
$$= 4.5 \times 10^{14} \frac{S_0}{AZ_1Z_2} \tau^2 e^{-\tau} \text{cm}^3 \text{s}^{-1}. \quad (12.21)$$

Here,

$$\tau = 3E_0/kT = 42.5(Z_1^2 Z_2^2 \mu/T_6)^{\frac{1}{3}}. \quad (12.22)$$

The maximum value of the integrand in the above equation is

$$I_{max} = \exp(-\tau). \quad (12.23)$$

The values of E_0, I_{max}, Δ, etc., apart from the Coulomb barrier for several reactions are tabulated in table 12.1 for $T_6 = 15$.

As the nuclear charge increases, the Coulomb barrier increases, and the Gamow peak E_0 also shifts toward higher energies. Note how rapidly the maximum of the integrand I_{max} decreases with the nuclear charge and the Coulomb barriers. The effective width Δ is a geometric mean of E_0 and kT, and $\Delta/2$ is much less rapidly varying between reactions (for $kT \ll E_0$). The rapid variation of I_{max} indicates that, of several nuclei present in the stellar core, the nuclear pairs with the smallest Coulomb barrier will have the largest reaction rates. The relevant nuclei will be consumed most rapidly at that stage. (Note, however, that for the p + p reaction, apart from the Coulomb barrier, the strength of the weak force, which transforms a proton to a neutron also comes into play.)

When nuclei of the smallest Coulomb barrier are consumed, there is a temporary dip in the nuclear generation rate, and the star contracts gravitationally until the temperature rises to a point where nuclei with the next lowest Coulomb barrier will start burning. At that stage, further contraction is halted. The star therefore goes through well-defined stages of different nuclear burning phases in its core at later epochs dictated by the height of the Coulomb barriers of the fuels. Note also from table 12.1, how far E_0, the effective

mean energy of reaction is below the Coulomb barrier at the relevant temperature. Stellar burning is so slow because the reactions are taking place at such a far sub-Coulomb region, and this is why the stars can last so long.

The above discussion assumes that a bare nuclear Coulomb potential is seen by the charged projectile. For nuclear reactions measured in the laboratory, the target nuclei are in the form of atoms with electron clouds surrounding the nucleus and giving rise to a screened potential—the total potential then goes to zero outside the atomic radius. The effect of the screening is to reduce the effective height of the Coulomb barrier. Atoms in the stellar interiors are in most cases in a highly stripped state, and nuclei are immersed in a sea of free electrons that tend to cluster near the nucleus. When the stellar density increases, the so called *Debye-Huckel radius* $R_D = (kT/4\pi e^2 \rho N_A \xi)^{1/2}$ (here $\xi = \sum_i (Z_i^2 + Z_i)X_i/A_i$), which is a measure of this cluster "radius," decreases, and the effect of shielding upon the reaction cross section becomes more important. This shielding effect enhances thermonuclear reactions inside the star. The enhancement factor $f_0 = \exp(0.188 Z_1 Z_2 \xi \rho^{1/2} T_6^{-3/2}$ varies between 1 and 2 for typical densities and compositions [Sal54] but can be large at high densities.

Therefore, the important ingredients to nucleosynthesis calculations are decay half-lives, electron and positron capture rates, photodisintegrations, neutrino-induced reaction rates, and strong interaction cross sections.

The solution of the above group of equations allows one to deduce the path for the r-process until reaching the heavier elements (see figure 12.9 below). The relative abundances of elements are also obtained theoretically by means of these equations using stellar models for the initial conditions, as the neutron density and the temperature vary.

12.5 The Sun

What are the nuclear processes that give rise to the huge thermonuclear energy of the sun, the latter having lasted 4.6×10^9 years (its assumed age)? It cannot be the simple fusion of two protons, or of α-particles, or even of protons with α-particles, since neither ${}_2^2\mathrm{He}$, ${}_4^8\mathrm{Be}$, nor ${}_3^5\mathrm{Li}$, is stable. The only possibility is proton-proton fusion in the form

$$\mathrm{p} + \mathrm{p} \rightarrow \mathrm{d} + \mathrm{e}^+ + \nu_e, \tag{12.24}$$

which occurs via β-decay, that is, due to the weak interaction. The cross section for this reaction for protons of energy around 1 MeV is very small, of the order of 10^{-23} b. The average lifetime of protons in the sun due to the transformation to deuterons by means of (12.24) is about 10^{10}y. This explains why the energy radiated from the sun is approximately constant in time, and not an explosive process.

Because of the low Coulomb barrier, in the p + p reaction ($E_c = 0.55$ MeV), a star like the sun would have consumed all its hydrogen quickly (note the relatively large value of $(\Delta) I_{\max}$ in table 12.1), were it not slowed down by the weakness of the weak interactions. The probability calculation for deuteron formation consists of two separate considerations: 1) penetration of a mutual potential barrier in a collision of two protons in a thermal bath

and 2) β-decay and positron and neutrino emission. Bethe and Critchfield [Bet38] used the original Fermi theory (point interaction) for the second part, which is adequate for the low energy process.

12.5.1 Deuterium formation

The total Hamiltonian H for the p-p interaction can be written as a sum of a nuclear term H_n and a weak interaction term H_w. As the weak interaction term is small compared to the nuclear term, first order perturbation theory can be applied, and Fermi's golden rule (chapter 6) gives the differential cross section as

$$d\sigma = \frac{2\pi\rho(E)}{\hbar v_i}|\langle f|H_w|i\rangle|^2. \tag{12.25}$$

Here $\rho(E) = dN/dE$, is the density of final states in the interval dE and v_i is the relative velocity of the incoming particles.

For a given volume V, the number of states dN between p and p + dp is

$$dN = dn_e dn_\nu = \left(V\frac{4\pi p_e^2 d\mathrm{p}_e}{h^3}\right)\left(V\frac{4\pi p_\nu^2 d\mathrm{p}_\nu}{h^3}\right). \tag{12.26}$$

By neglecting the recoil energy of deuterium (since this is much heavier than the outgoing positron in the final state) and neglecting the mass of the electron neutrino, we have $E = E_e + E_\nu = E_e + c\mathrm{p}_\nu$ and $dE = dE_\nu = c\mathrm{p}_\nu$, for a given E_e, and,

$$\rho(E) = dN(E)/dE = dn_e(dn_\nu/dE) = 16\pi^2V^2/(c^3h^6)\mathrm{p}_e^2(E - E_e)^2 d\mathrm{p}_e = \rho(E_e)d\mathrm{p}_e. \tag{12.27}$$

The matrix element that appears in the differential cross section may be written in terms of the initial state wavefunction Ψ_i of the two protons in the entrance channel and the final state wavefunction[1] Ψ_f as

$$H_{if} = \int |\Psi_d\Psi_e\Psi_\nu|^* H_\beta \Psi_i d\tau. \tag{12.28}$$

If the energy of the electron is large compared to $Z \times$ Rydberg (Rydberg $R_\infty = 2\pi^2me^4/ch^3$), then a plane wave approximation is a good one, $\Psi_e = 1/(\sqrt{V})\exp(i\mathbf{k_e}\cdot\mathbf{r})$, where the wavefunction is normalized over volume V. For lower energies, typically 200 keV or less, the electron wavefunction could be strongly affected by nuclear charge. Apart from this, the final state wavefunction $|\Psi_d\Psi_e\Psi_\nu|$ has a deuteron part Ψ_d whose radial part rapidly vanishes outside the nuclear domain R_0, so that the integration need not extend much beyond $r \simeq R_0$ (for example, the deuteron radius $R_d = 1.7$ fm). Note that because of the Q-value of 0.42 MeV for the reaction, the kinetic energy of the electron ($K_e \leq 0.42$ MeV) and the average energy of the neutrinos ($\bar{E}_\nu = 0.26$ MeV) are low enough that, for both electrons and neutrino wavefunctions, the product $kR_0 \leq 2.2 \times 10^{-3}$, and the exponential can be approximated by the first term of the Taylor expansion

$$\Psi_e = 1/(\sqrt{V})|1 + i(\mathbf{k_e}\cdot\mathbf{r})| \sim 1/(\sqrt{V}), \tag{12.29}$$

[1] The same arguments were used in chapter 8 in connection with Fermi's theory for β-decay.

and

$$\Psi_{\nu} \sim 1/(\sqrt{V}). \tag{12.30}$$

Then the expectation value of the Hamiltonian, given a strength of interaction governed by the coupling constant g, is

$$H_{if} = \int [\Psi_d \Psi_e \Psi_\nu]^* H_{ft} \Psi_i d\tau = \frac{g}{V} \int [\Psi_d]^* \Psi_i d\tau. \tag{12.31}$$

The integration over $d\tau$ can be broken into a space part M_{space} and a spin part M_{spin}, so that the differential cross section is

$$d\sigma = \frac{2\pi}{h\nu_i} \frac{16\pi^2}{c^3 h^6} g^2 M^2_{\text{spin}} M^2_{\text{space}} p_e^2 (E - E_e)^2 dp_e. \tag{12.32}$$

Thus the total cross section up to an electron energy of E can be obtained by integration as proportional to

$$\int_0^E \mathrm{p}_e^2 (E - E_e)^2 d\mathrm{p}_e = \frac{(m_e c^2)^5}{c^3} \int_1^W (W_e^2 - 1)^{1/2} (W - W_e)^2 W_e dW_e, \tag{12.33}$$

where $W = (E + m_e c^2)/m_e c^2$.

The integral over W becomes

$$f(W) = (W^2 - 1)^{1/2} \left[\frac{W^4}{30} - \frac{3W^2}{20} - \frac{2}{15} \right] + \frac{W}{4} \ln \left[W + (W^2 - 1)^{1/2} \right], \tag{12.34}$$

so that

$$\sigma = \frac{m_e^5 c^4}{2\pi^3 h^7} f(W) g^2 M^2_{\text{space}} M^2_{\text{spin}}. \tag{12.35}$$

At large energies, the factor $f(W)$ behaves as

$$f(W) \propto W^5 \propto \frac{1}{30} E^5. \tag{12.36}$$

In the process that we are considering, $\mathrm{p} + \mathrm{p} \rightarrow \mathrm{d} + \mathrm{e}^+ + \nu_\mathrm{e}$, the final state nucleus (deuterium in its ground state) has $J_f^\pi = 1^+$, with a predominant relative orbital angular momentum $l_f = 0$ and $S_f = 1$ (triplet S-state). For a maximum probability of the process, called the super-allowed transition, there are no changes in the *orbital* angular momentum between the initial and final states of the nuclei. Hence for super-allowed transitions, the initial two interacting protons in the $\mathrm{p} + \mathrm{p}$ reaction that we are considering must have $l_i = 0$. Since the two protons are identical particles, the Pauli principle requires $S_i = 0$, so that the total wavefunction will be antisymmetric in space and spin coordinates. Thus, we have a process:

$$|S_i = 0, l_i = 0\rangle \rightarrow |S_f = 1, l_f = 0\rangle. \tag{12.37}$$

This is a pure Gamov-Teller transition with the coupling constant g = g_a due to the axial vector component.

The spin matrix element in the above expression for the energy-integrated cross section σ is obtained from summing over the final states, averaging over the initial states, and dividing by 2 to take into account that we have two identical particles in the initial state. Thus,

$$\lambda = \frac{1}{\tau} = \frac{m^5c^4}{2\pi^3\hbar^7\nu_i} f(W)g^2 \frac{M^2_{\text{space}} M^2_{\text{spin}}}{2}, \tag{12.38}$$

where, $M^2_{\text{spin}} = \frac{(2J+1)}{(2J_1+1)(2J_2+1)} = 3$. And the space matrix element is

$$M_{\text{space}} = \int_0^\infty \chi_f(r)\chi_i(r)r^2dr, \tag{12.39}$$

in units of $\text{cm}^{3/2}$.

The above integral contains the radial parts of the nuclear wavefunctions $\chi(r)$, and involves Coulomb wavefunctions for barrier penetration at (low) stellar energies. The integral can be evaluated by numerical methods. In the overlap integral one needs only the *S*-wave part for the wavefunction of the deuteron ψ_d, as the *D*-wave part makes no contribution to the matrix element [Fri51], although its contribution to the normalization has to be accounted for. The wavefunction of the initial two-proton system ψ_p is normalized to a plane wave of unit amplitude, and again only the *S*-wave part is needed. The asymptotic form of ψ_p (well outside the range of nuclear forces) is given in terms of regular and irregular Coulomb functions and has to be defined through quantities related to the *S*-wave phase shifts in p-p scattering data). The result is a minuscule total cross section of $\sigma = 10^{-47}\text{cm}^2$ at a laboratory beam energy of $E_p = 1$ MeV, which cannot be measured experimentally even with milliampere beam currents.

The reaction $\text{p} + \text{p} \rightarrow \text{d} + \text{e}^+ + \nu_e$ is a nonresonant reaction, and at all energies the rate varies smoothly with energy (and with stellar temperatures), with $S(0) = 3.8 \times 10^{-22}$ keV barn and $dS(0)/dE = 4.2 \times 10^{-24}$ barn. At, for example, the central temperature of the sun $T_6 = 15$, this gives $\langle\sigma\nu\rangle_{pp} = 1.2 \times 10^{-43}\ \text{cm}^3\ \text{s}^{-1}$. For density in the center of the sun $\rho = 100\ \text{gm cm}^{-3}$ and equal mixture of hydrogen and helium ($X_H = X_{He} = 0.5$), the mean life of a hydrogen nucleus against conversion to deuterium is $\tau_H(\text{H}) = 1/N_H\langle\sigma\nu\rangle_{pp} \sim 10^{10}$yr. This is comparable to the age of the old stars. The reaction is so slow primarily because of weak interactions and to a lesser extent because of the smallness of the Coulomb barrier penetration factor (which contributes a factor $\sim 10^{-2}$ in the rate), and is the primary reason why stars consume their nuclear fuel of hydrogen so slowly.

12.5.2 Deuterium burning

Once deuterium is produced in the weak interaction-mediated p + p reaction, the main way this is burned in the sun turns out to be

$$\text{d} + \text{p} \rightarrow {}^3\text{He} + \gamma. \tag{12.40}$$

This is a nonresonant direct capture reaction to the 3He ground state with a Q-value of 5.497 MeV and S(0) = 2.5 x 10**(-3) keV-barn. The angle averaged cross sections measured

as a function of proton + deuterium center of mass energy, where the capture transitions were observed in γ-ray detectors at several angles to the incident proton beam direction, are well explained by the direct capture model.

The reactions comprising the rest of the (three) pp chains start out with the predominant product of deuterium burning: ^{3}He (manufactured from d + p reaction) as the starting point. The only other reactions with a $S(0)$ greater than the above are d(d, p)t, d(d, n)^{3}He, d(^{3}He, p)^{4}He, and d(^{3}He, γ)^{5}Li. However, because of the overwhelmingly large number of protons in the stellar thermonuclear reactors, the process involving protons on deuterium dominates. The rate of this reaction is so fast compared to its precursor, $p + p \rightarrow d + e^+ \nu_e$, that the overall rate of the pp chain is not determined by this reaction.

One can show that the abundance ratio of deuterium to hydrogen in a quasi-equilibrium has an extremely small value, signifying that deuterium is destroyed in thermonuclear burning. The time dependence of deuterium abundance D is

$$\frac{dD}{dt} = r_{pp} - r_{pd} = \frac{H^2}{2}\langle\sigma v\rangle_{pp} - HD\langle\sigma v\rangle_{pd}. \tag{12.41}$$

The self-regulating system eventually reaches a state of quasi-equilibrium and has

$$(D/H) = \langle\sigma v\rangle_{pp}/(2\langle\sigma v\rangle_{pd}) = 5.6 \times 10^{-18}, \tag{12.42}$$

at $T_6 = 5$ and 1.7×10^{-18} at $T_6 = 40$. For the solar system however, this ratio is 1.5×10^{-4} and the observed $(D/H)_{obs}$ ratio in the cosmos is $\sim 10^{-5}$. The higher cosmic ratio is due to primordial nucleosynthesis in the early phase of the universe before the stars formed. (The primordial deuterium abundance is a key quantity used to determine the baryon density in the universe). Stars only destroy the deuterium in their core due to the above reaction.

12.5.3 ^{3}He burning

The ppI chain is completed (see figure 12.5) through the burning of ^{3}He via the reaction

$$^3\text{He} + {}^3\text{He} \rightarrow p + p + {}^4\text{He}, \tag{12.43}$$

with an S-factor $S(0) = 5500$ keV barn and Q-value = 12.86 MeV. In addition, the reaction

$$^3\text{He} + D \rightarrow {}^4\text{He} + p \tag{12.44}$$

has an S-factor $S(0) = 6240$ keV barn, but since the deuterium concentration is very small as argued above, the first reaction dominates the destruction of ^{3}He even though both reactions have comparable $S(0)$ factors.

^{3}He can also be consumed by reactions with ^{4}He (the latter is preexisting from the gas cloud from which the star formed and is synthesized in the early universe and in population III objects). These reactions proceed through direct captures and lead to the ppII and ppIII parts of the chain (happening 15% of the time). Note that the reaction ^{4}He(α, γ)^{7}Be and the subsequent reaction ^{7}Be(p, γ)^{8}B control the production of high energy neutrinos in the sun and are particularly important for the ^{37}Cl solar neutrino detector constructed by Ray Davis and collaborators [Bah89].

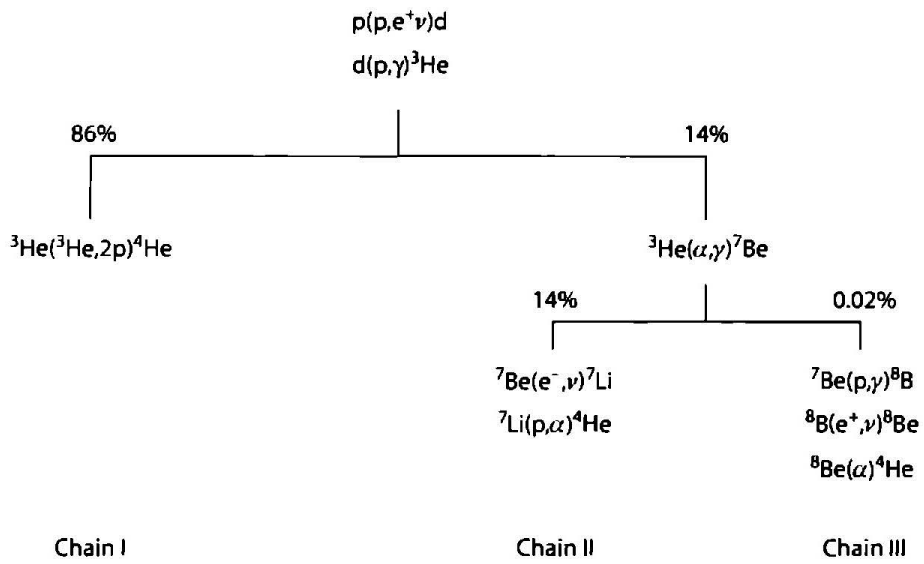

Figure 12.5 The p-p chain reaction (p-p cycle). The percentages for the several branches are calculated for the center of the sun [Bah89].

12.5.4 *Reactions involving ^{7}Be*

As shown in figure 12.5, about 14% of the time, ^{3}He is burned with ^{4}He radiatively to ^{7}Be. Subsequent reactions involving ^{7}Be as a first step in alternate ways complete the fusion process: $4H \rightarrow {}^4He$ in the ppII and ppIII chains.

Electron capture

The first step of the ppII chain is the electron capture reaction on ^{7}Be : $^7Be + e^- \rightarrow {}^7Li + \nu_e$. This decay goes both to the ground state of ^{7}Li and to its first excited state at $E_X = 0.478$ keV, $J^\pi = \frac{1}{2}^-$)—the percentage of decays to the excited state being 10.4 % in the laboratory. The energy released in the reaction with a Q-value of 0.862 keV is carried away by escaping monoenergetic neutrinos with energies $E_\nu = 862$ and 384 keV. The measured laboratory mean life of the decay is $\tau = 76.9$d.

The capture rate in the laboratory can be obtained from Fermi's golden rule and utilizing the fact that the wavefunctions of both the initial and the final nucleus vanish rapidly outside the nuclear domain. The electron wavefunction in that domain. The approximated as its value at $r = 0$ and the neutrino wavefunction by a plane wave normalized to volume V, so that $H_{if} = \Psi_e(0)g/\sqrt{V}\int \Psi^*_{^7\mathrm{Li}}\Psi_{^7\mathrm{Be}}d\tau = \Psi_e(0)gM_n/\sqrt{V}$, where M_n represents the nuclear matrix element and the resultant capture rate is

$$\lambda_{\mathrm{EC}} = \frac{1}{\tau_{\mathrm{EC}}} = \frac{g^2M_n^2}{\pi c^3\hbar^4}E_\nu^2|\Psi_e(0)|^2. \tag{12.45}$$

In the laboratory capture process, any of the various electron shells contribute to the capture rate; however the K shell gives the dominant contribution. At temperatures inside the sun, for example, $T_6 = 15$, nuclei such as ^{7}Be are largely ionized. The nuclei, however, are immersed in a sea of free electrons resulting from the ionized process, and therefore electron capture from continuum states is possible. Since all factors in the capture of

continuum electrons in the sun are approximately the same as those in the case of atomic electron capture, except for the respective electron densities, the ^{7}Be lifetime in a star, τ_{fr} is related to the terrestrial lifetime τ_t by

$$\frac{\tau_{fr}}{\tau_t} \sim \frac{2|\Psi_t(0)|^2}{|\Psi_{fr}(0)|^2}, \tag{12.46}$$

where $|\Psi_{fr}(0)|^2$ is the density of the free electrons $n_e = \rho/m_H$ at the nucleus, ρ being the stellar density. The factor of 2 in the numerator takes care of the two spin states of calculation of the λ_t, whereas the corresponding λ_{fr} is calculated by averaging over these two orientations.

Taking account of distortions of the electron wavefunctions due to the thermally averaged Coulomb interaction with nuclei of charge Z and contribution due to hydrogen (of mass fraction X_H) and heavier nuclei, one gets the continuum capture rate as

$$\tau_{fr} = \frac{2|\Psi_t(0)|^2\tau_t}{(\rho/M_H)[(1 + X_H)/2]2\pi Z\alpha(m_e c^2/3kT)^{1/2}}, \tag{12.47}$$

with $|\Psi_e(0)|^2 \sim (Z/a_0)^3/\pi$. Bahcall et al. [Bah69] obtained for the ^{7}Be nucleus a lifetime

$$\tau_{fr}(^7\text{Be}) = 4.72 \times 10^8 \frac{T_6^{1/2}}{\rho(1 + X_H)}\text{s}. \tag{12.48}$$

The temperature dependence comes from the nuclear Coulomb field corrections to the electron wavefunction, which are thermally averaged. For solar conditions the above rate [Bah69b] gives a continuum capture rate of $\tau_{fr}(^7\text{Be}) = 140$ d as compared to the terrestrial mean life of $\tau_t = 76.9$ d. Actually, under stellar conditions, there is a partial contribution from some ^{7}Be atoms which are only partially ionized, leaving electrons in the inner K shell. So the contributions of such partially ionized atoms have to be taken into account. Under solar conditions the K shell electrons from partially ionized atoms give another 21% increase in the total decay rate. Including this, gives the solar lifetime of a ^{7}Be nucleus as $\tau_\odot(^7\text{Be}) = 120$ d. In addition, the solar fusion reactions have to be corrected for plasma electrostatic screening enhancement effects.

Formation of ^{8}B

Apart from the electron capture reaction, the ^{7}Be that is produced is partly consumed by proton capture via $^7\text{Be}(p,\alpha)^8\text{B}$ reaction. Under solar conditions, this reaction happens only 0.02% of the time. The proton capture on ^{7}Be proceeds at energies away from the 640 keV resonance via the direct capture process. Since the product ^{7}Li nucleus emits an intense γ-ray flux of 478 keV, this prevents the direct measurement of the direct capture to ground state γ-ray yield. The process is studied indirectly by either the delayed positron or the breakup of the product ^{8}B nucleus into two α-particles. This reaction has a weighted average $S(0) = 0.0238$ keV barn [Fil83].

The product ^{8}B is a radioactive nucleus that decays with a lifetime r = 1.1 s

$$^8\text{B} \rightarrow {}^8\text{Be} + e^+ + \nu_e. \tag{12.49}$$

The positron decay of $^8B(J^\pi = 2^+)$ goes mainly to the $\Gamma = 1.6$ MeV broad excited state in ^8Be at excitation energy $E_x = 2.94$ MeV $(J^\pi = 2^+)$ due to the selection rules. This excited state has a very short lifetime and quickly decays into two α-particles. This completes the ppIII part of the pp chain. The average energy of the neutrinos from ^8B reactions is $\bar{E}_\nu(^8B) = 7.3$ MeV. These neutrinos, having relatively high energy, play an important role in several solar neutrino experiments.

12.6 The CNO Cycle

The sun gets most of its energy generation through the pp chain reactions (see figure 12.7). However, as the central temperature (in stars more massive than the sun) gets higher, the CNO cycle (see below for reaction sequence) comes to dominate over the pp chain at T_6 near 20 (this changeover assumes the solar CNO abundance; the transition temperature depends upon CNO abundance in the star).

The early generation of stars (usually referred to as the Population II or Pop II stars, although there is an even earlier generation of Pop III stars) generated energy primarily through the pp chain. These stars are still shining in globular clusters, and being of mass lower than that of the sun, are very old. Most other stars that we see today are later generation stars formed from the debris of heavier stars that contained heavy elements apart from (the most abundant) hydrogen. Thus in second and third generation stars (which are slightly heavier than the sun), where higher central temperatures are possible because of higher gravity, hydrogen burning can take place through faster chains of reactions involving heavy elements C, N, and O which have some reasonable abundance (exceeding 1%)) compared to other heavy elements like Li, Be, B, which are extremely low in abundance. The favored reactions involve heavier elements (than those of the pp chain), which have the smallest Coulomb barriers but with reasonably high abundance. Even though the Coulomb barriers of Li, Be, B are smaller than those of C, N, O (when protons are the lighter reactants (projectiles)), they lose out due to their lower abundance.

In 1937–1938, Bethe and von Weizsäcker independently suggested the CN part of the cycle, which goes as (see figure 12.6)

$$^{12}C(p,\gamma)^{13}N(e^+\nu_e)^{13}C(p,\gamma)^{14}N(p,\gamma)^{15}O(e^+\nu)^{15}N(p,\alpha)^{12}C. \tag{12.50}$$

This has the net result, as before, $4p \rightarrow {}^4He + 2e^+ + 2\nu_e$ with $Q = 26.73$. In these reactions, the ^{12}C and ^{14}N act merely as catalysts as their nuclei are "returned" at the end of the cycle. Therefore the ^{12}C nuclei act as seeds that can be used over and over again, even though the abundance of the seed material is minuscule compared to that of the hydrogen. Note that a loss of the catalytic material from the CN cycle takes place through the $^{15}N(p,\gamma)^{16}O$ reactions. However, the catalytic material is subsequently returned to the CN cycle by the reaction $^{16}O(p,\gamma)^{17}F(e^+\nu_e)^{17}O(p,\alpha)^{14}N$.

In the CN cycle (see figure 12.6), the two neutrinos involved in the β-decays (of ^{13}N $(t_{1/2} = 9.97\text{min})$ and ^{15}O $(t_{1/2} = 122.24\text{s})$) are of relatively low energy, and most of the total energy $Q = 26.73$ MeV from the conversion of four protons into helium is deposited in the

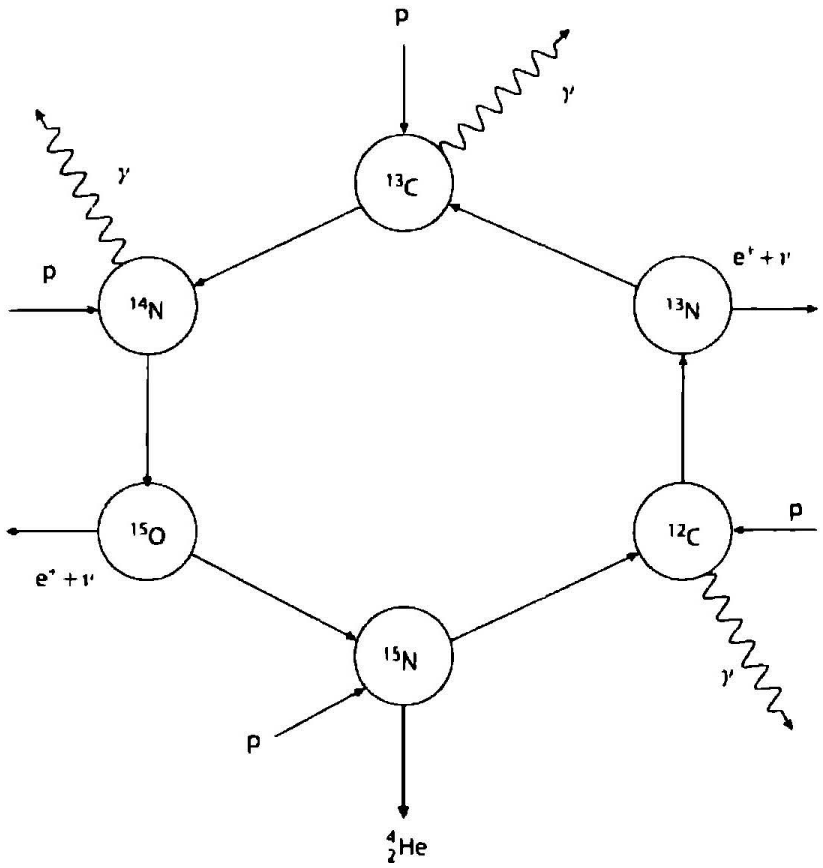

Figure 12.6 The CNO cycle [Bet38].

stellar thermonuclear reactor. The rate of the energy production is governed by the slowest thermonuclear reaction in the cycle. Here nitrogen isotopes have the highest Coulomb barriers in charged particle reactions, because their $Z = 7$. Among them $^{14}N(p,\gamma)^{15}O$ is the slowest because this reaction, having a final state photon, is governed by electromagnetic forces while that involving the other nitrogen isotope: $^{15}N(p,\alpha)^{12}C$ is governed by strong forces and is therefore faster.

From the CN cycle, there is actually a branching off from ^{15}N by the reaction $^{15}N(p,\gamma)^{16}O$ mentioned above. This involves isotopes of oxygen and is called the ON cycle; finally the nitrogen is returned to the CN cycle through ^{14}N. Together, the CN and ON cycles constitutes the CNO bi-cycle. The two cycles differ considerably in their relative cycle rates: the ON cycle operates only once for every 1000 cycles of the main CN cycle. This can be gauged from the $S(0)$ factors of the two sets of reactions branching off from ^{15}N: for the $^{15}N(p,\alpha)^{12}C$ reaction $S(0) = 65$ MeV b, whereas for $^{15}N(p,\gamma)^{16}O$, it is 64 keV b, a factor of 1000 smaller.

12.6.1 Hot CNO and rp process

The above discussion of the CNO cycle is relevant for typical temperatures $T_6 \geq 20$. These are found in quiescently hydrogen burning stars with solar composition which are only slightly more massive than the sun. There are situations where the hydrogen burning takes

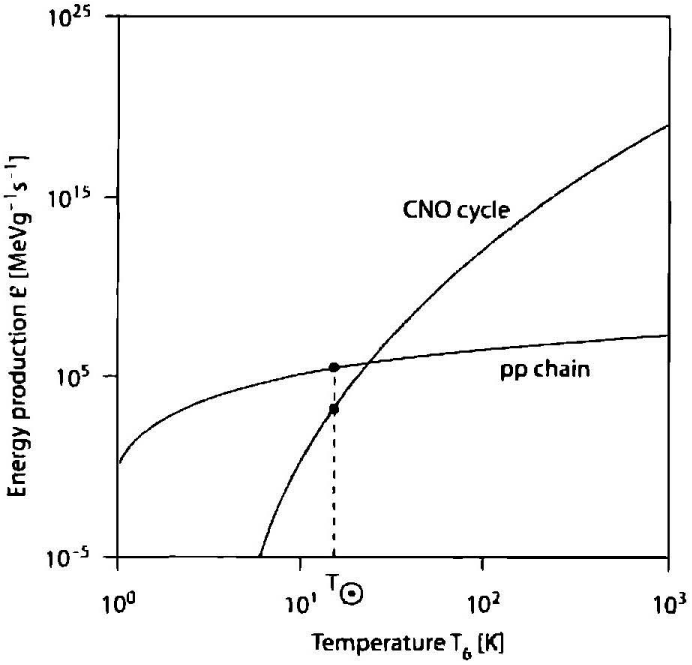

Figure 12.7 Comparison of the energy production in the pp and in the CNO cycle as a function of the star temperature [Ib65].

place at temperatures ($T \sim 10^8$–10^9 K), far in excess of those found in the interiors of the ordinary "main sequence" stars. Examples of these are hydrogen burning at the accreting surface of a neutron star or in the explosive burning on the surface of a white dwarf, that is, novae, or the outer layers of a supernova shock heated material in the stellar mantle.

These hot CNO cycles operate under such conditions on a rapid enough timescale (a few seconds) so that even "normally" β-unstable nuclei like ^{13}N will live long enough to be burned by thermonuclear charged particle reactions, before they are able to β-decay. So, unlike the normal CNO the amount of hydrogen to helium conversion in hot CNO is limited by the β-decay lifetimes of the proton-rich nuclei like ^{14}O and ^{15}O rather than the proton capture rate of ^{14}N. For temperatures, $T \geq 5 \times 10^8$K, nucleosynthesised material can leak out of the cycles. This leads to a diversion from lighter to heavier nuclei and is known as the rapid proton capture or rp process.

The nucleosynthesis path of the rp process of rapid proton addition is analogous to the r process of neutron addition. The hot hydrogen bath converts CNO nuclei into isotopes near the region of proton unbound nuclei (the proton drip line). For each neutron number, a maximum mass number A is reached where the proton capture must wait until β^+-decay takes place before the buildup of heavier nuclei (for an increased neutron number) can take place. Unlike the r process the rate of the rp process is increasingly hindered due to the increasing Coulomb barrier of heavier and higher-Z nuclei to proton projectiles. Thus the rp process does not extend all the way to the proton drip line but runs close to the β-stability valley and runs through where the β^+-decay rate compares favorably with the proton captures. A comparison of the reaction paths of rp and r processes in the (N, Z) plane is given in figure 12.9.

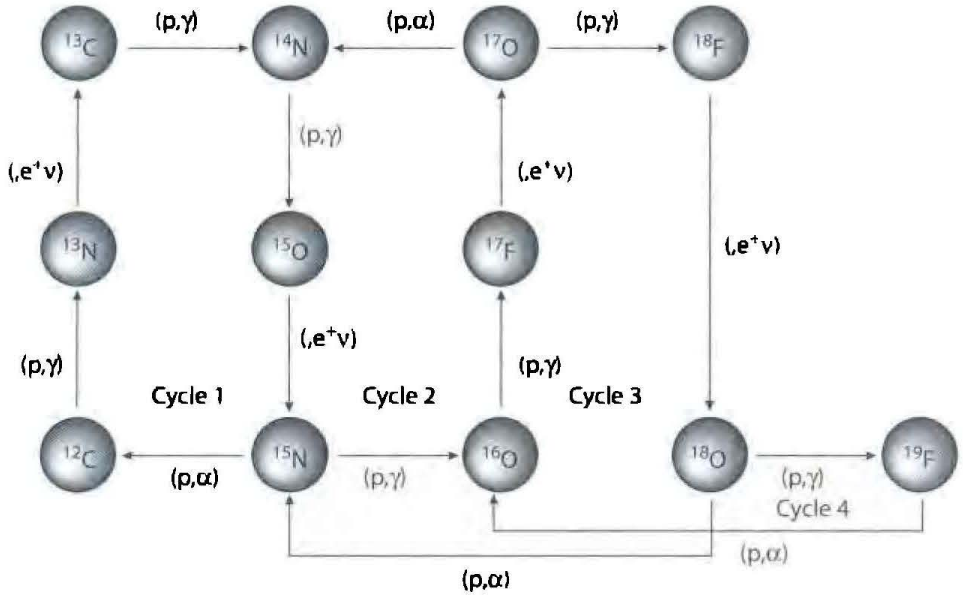

Figure 12.8 The various CNO cycles. The left part is the CN cycle where only C and N serve as catalysis for the conversion of four protons into ^{4}He. Here the slowest fusion reaction is the (p,γ) reaction on ^{14}N, whereas the slower β-decay has a half-life of 9.97m. In the CNO cycle 2 (middle), there is leakage from the CN cycle to the ON cycle through the branching at ^{15}N. The flow is returned to the CN cycle (which cycles 1000 times for each ON cycle) through $^{17}O(p,\alpha)^{14}N$. The right part represents additional cycles linking into the CNO cycle through the $^{17}O(p,\gamma)^{18}F$ reaction [courtesy of Frank Timmes].

12.7 Helium Burning

After hydrogen burning in the core of the star has exhausted its fuel, the helium core contracts slowly. Its density and temperature go up as gravitational energy released is converted to internal kinetic energy. The contraction also heats hydrogen at the edge of the helium core, igniting the hydrogen to burn in a shell. At a still later stage in the star's evolution, the core has contracted enough to reach central temperature density conditions: $T_6 = 100$–200 and $\rho_c = 10^2$–10^5 gm cm^{-3} when the stellar core settles down to burn ^{4}He in a stable manner. The product of helium burning is ^{12}C. Since in nature the $A = 5$ and $A = 8$ nuclei are not stable, the question arises as to how helium burning bridges this gap. A direct interaction of three α-particles to produce a ^{12}C nucleus ($\alpha + \alpha + \alpha \rightarrow {}^{12}C$) would seem at first sight, to be too improbable (as was mentioned, for example, in Bethe's 1939 paper [Bet39], which was primarily on the CN cycle). However, Öpik [Opi51] and Salpeter [Sal52, Sal57] independently proposed a two-step process where in the first step, two α-particles interact to produce a ^{8}Be nucleus in its ground state (which is unstable to α breakup), followed by the unstable nucleus interacting with another α-particle process to produce a ^{12}C nucleus.

Thus the triple-α reaction begins with the formation of ^{8}Be that has a lifetime of only 1×10^{-16} s (this is found from the width $\Gamma = 6.8$ eV of the ground state and is the cause of the $A = 8$ mass gap). This is, however, long compared to the transit time 1×10^{-19} s of two α-particles to scatter past each other nonresonantly with kinetic energies comparable to the Q-value of the reaction namely, $Q = -92.1$ keV. So it is possible to have an equilibrium

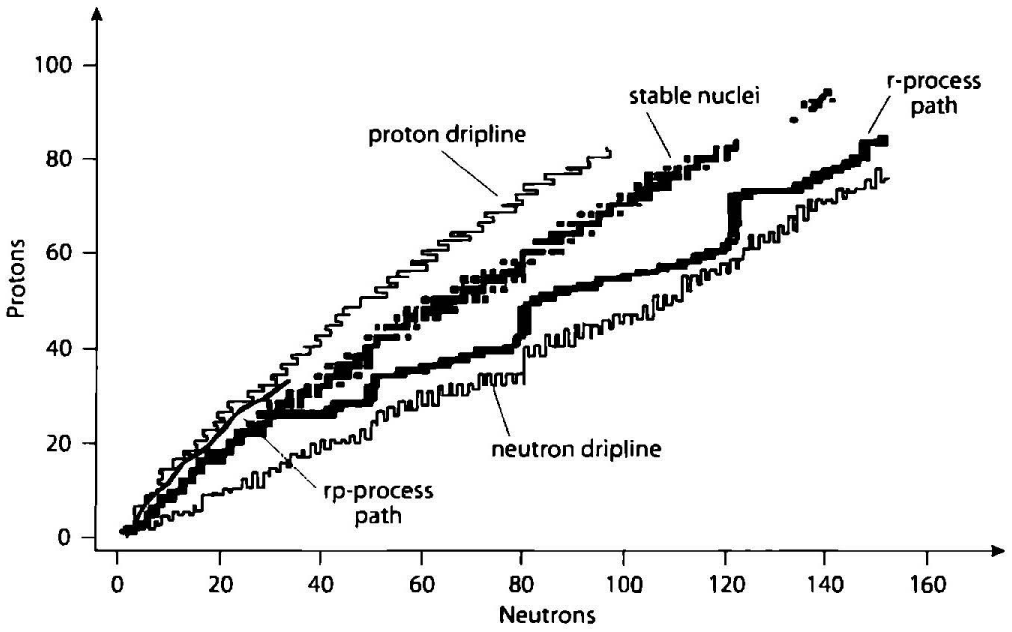

Figure 12.9 Schematic paths of the r process and rp process in the N, Z-plane with respect to the valley of β stability and the neutron drip and proton drip lines.

build-up of a small quantity of ^{8}Be in equilibrium with its decay or reaction products $\alpha + \alpha \rightarrow {}^8$Be. The equilibrium concentration of the ^{8}Be nucleus can be calculated through the Saha equation

$$N_{12} = \frac{N_1 N_2}{2} \left(\frac{2\pi}{\mu kT} \right)^{3/2} h^3 \frac{(2J+1)}{(2J_1+1)(2J_2+1)} \exp\left(-\frac{E_R}{kT} \right), \tag{12.51}$$

at the relevant temperature $T_6 = 11$ and $\rho = 10^5$ gm cm^{-3} to be

$$\frac{N(^8\text{Be})}{N(^4\text{He})} = 5.2 \times 10^{-10}. \tag{12.52}$$

Salpeter suggested that this small quantity of ^{8}Be serves as the seed for the second stage of the triple-α capture into the ^{12}C nucleus. It was, however, shown by Hoyle [Hoy53] that the amount of ^{12}C produced for the conditions inside a star at the tip of the red-giant branch is insufficient to explain the observed abundance, *unless* the reaction proceeds through a resonance process [Hoy54]. The presence of such a resonance greatly speeds up the rate of the triple-α process, which then proceeds through an s-wave ($l = 0$) resonance in ^{12}C near the threshold of the ^{8}Be + α reaction. Since ^{8}Be and ^{4}He both have $J^\pi = 0^+$, an s-wave resonance would imply that the resonant state in question has to be 0^+ in the ^{12}C nucleus.

Hoyle suggested the excitation energy to be: $E_X \sim 7.68$ MeV in the ^{12}C nucleus, and this state was experimentally found by W.A. Fowler's group [Coo57] with spin-parity $J^\pi = 0^+$. This state has a total width [RR88] $\Gamma = 8.9 \pm 1.08$ eV, most of which lies in Γ_α, due to the major propensity of the ^{12}C nucleus to break up through α-decay. (The decay of the excited state of ^{12}C by γ-rays cannot go directly to the ground state, since the resonance state as well as the ground state of the ^{12}C nucleus have both $J^\pi = 0^+$ and $0^+ \rightarrow 0^+$ decays forbidden. This partial width due to γ-decay is several thousand times smaller than that

due to α-decay). So, $\Gamma = \Gamma_\alpha + \Gamma_{\rm rad} \sim \Gamma_\alpha$ and $\Gamma_{\rm rad} = \Gamma_\gamma + \Gamma_{e^+e^-} = 3.67 \pm 0.50$ meV. Again the radiative width $\Gamma_{\rm rad}$ is dominated by the width due to photon width deexcitation: $\Gamma_\gamma = 3.58 \pm 0.46$ meV. (Note the scales of *milli*electron volts.)

The reaction rate for the ^{12}C formation can be calculated by using the properties of the resonant state and the thermally averaged cross section

$$r_{1\alpha} = N_{^8\mathrm{Be}} N_\alpha \langle \sigma v \rangle_{^8\mathrm{Be}+\alpha}. \tag{12.53}$$

Here $N_{^8\mathrm{Be}}$ and N_α are the number densities of interacting ^{8}Be and ^{4}He nuclei and the angular brackets denote thermal averaging over a Maxwell-Boltzmann distribution $\psi(E)$. This averaging leads to

$$r_{1\alpha} = N_{^8\mathrm{Be}} N_\alpha \int_0^\infty \psi(E) v(E) \sigma(E) dE. \tag{12.54}$$

with

$$\psi(E) = \frac{2}{\sqrt{\pi}} \frac{E}{kT} \exp(-E/kT) \frac{dE}{(kTE)^{1/2}}, \tag{12.55}$$

and

$$\sigma(E) = \pi \left(\frac{\lambda}{2\pi} \right)^2 \frac{2J+1}{(2J_1+1)(2J_2+1)} \frac{\Gamma_1 \Gamma_2}{(E-E_R)^2 + (\Gamma/2)^2} \tag{12.56}$$

is the Breit-Wigner resonant reaction cross section with the resonant energy centroid at $E = E_R$. The total width Γ is a sum of all decay channel widths such as $\Gamma_1 = \Gamma_\alpha$ and $\Gamma_2 = \Gamma_\gamma$.

If the width Γ is only a few eV, then the functions $\psi(E)$ and $v(E)$ can be pulled out of the integral. Then the reaction rate will contain an integral like $\int_0^\infty \sigma_{BW}(E) dE = 2\pi(\lambda/2\pi\hbar)^2 \omega \Gamma_1 \Gamma_2 / \Gamma$, where $\omega = (2J+1)/|(2J_1+1)(2J_2+1)|$, and the functions pulled out of the integral need to be evaluated at $E = E_R$. Since most of the time the excited state of the ^{12}C* breaks up into α-particles, we have $\Gamma_1 = \Gamma_\alpha$ dominating over Γ_γ and $(\Gamma_1 \Gamma_2 / \Gamma) \sim \Gamma_2$. This limit usually holds for resonances of energy sufficiently high that the incident particle width (Γ_1) dominates the natural width of the state (Γ_2). In that case, we can use the number density of the ^{8}Be nuclei in equilibrium with the α-particle nuclei bath as described by the Saha equilibrium condition

$$N(^8\mathrm{Be}) = N_\alpha^2 \omega f \frac{h^3}{(2\pi\mu kT)^{3/2}} \exp(-E_r/kT), \tag{12.57}$$

where f is the screening factor.

It is possible to get the overall triple-α reaction rate by calculating the equilibrium concentration of the excited (resonant) state of ^{12}C reached by the $^8\mathrm{Be} + \alpha \rightarrow {}^{12}\mathrm{C}^*$ reaction and then multiplying that concentration by the γ-decay rate $\Gamma_\gamma/\hbar$ which leads to the final product of ^{12}C. So the reaction rate for the final step of the triple-α reaction turns out to be

$$r_{1\alpha} = N_{^8\mathrm{Be}} N_\alpha \hbar^2 \left(\frac{2\pi}{\mu kT} \right)^{3/2} \omega f \Gamma_2 \exp(-E_r'/kT), \tag{12.58}$$

where μ is the reduced mass of the reactants ^{8}Be and α-particle. This further reduces by the above argument to

$$r_{3\alpha\to^{12}C} = \frac{N_\alpha^3}{2} 3^{3/2} \left(\frac{2\pi\hbar^2}{M_\alpha kT}\right)^3 f \frac{\Gamma_\alpha\Gamma_\gamma}{\Gamma\hbar} \exp\left(-\frac{Q}{kT}\right). \tag{12.59}$$

The Q-value of the reaction is the sum of $E_R(^8\text{Be}+\alpha) = 287$ keV and $E_R(\alpha+\alpha) = |Q| = 92$ keV and turns out to be $Q_{3\alpha} = (M_{^{12}C^*} - 3M_\alpha)c^2 = 379.38 \pm 0.20$ keV. Numerically, the energy generation rate for the triple-α reaction is

$$\epsilon_{3\alpha} = \frac{r_{3\alpha}Q_{3\alpha}}{\rho} = 3.9\times10^{11}\frac{\rho^2 X_\alpha^3}{T_8^3} f \exp(-42.94/T_8) \text{ erg gm}^{-1}\text{ s}^{-1}. \tag{12.60}$$

The triple-α reaction has a very strong temperature dependence near a value of temperature T_0, and one can show that the energy generation rate is

$$\epsilon(T) = \epsilon(T_0)\left(\frac{T}{T_0}\right)^n, \tag{12.61}$$

where $n = 42.9/T_8 - 3$. Thus at a sufficiently high temperature and density, the helium gas is very highly explosive, so that a small temperature rise gives rise to greatly accelerated reaction rate and energy liberation. When helium thermonuclear burning is ignited in the stellar core under degenerate conditions, an unstable and sometimes explosive condition develops.

12.8 Red Giants

The product of the triple-α reactions, ^{12}C, is burned into ^{16}O by α-capture reactions

$$^{12}\text{C} + \alpha \to {}^{16}\text{O} + \gamma. \tag{12.62}$$

If this reaction proceeds too efficiently, then all the carbon will be burned up to oxygen. Carbon is, however, the most abundant element in the universe after hydrogen, helium, and oxygen, and the cosmic C/O ratio is about 0.6. In fact, the O and C burning reactions and the conversion of He into C and O take place in similar stellar core temperature and density conditions. Major ashes of He burning in red giant stars are C and O. Red giants are the source of the galactic supply of ^{12}C and ^{16}O. Fortuitous circumstances of the energy level structures of these α-particle nuclei are in fact important for the observed abundance of oxygen and carbon.

For example, if as in the case of the triple-α reaction, there were a resonance in the $^{12}\text{C}(\alpha,\gamma)^{16}\text{O}$ reaction near the Gamow window for He burning conditions ($T_9 \sim 0.1 - 0.2$), then the conversion $^{12}\text{C}\to{}^{16}\text{O}$ would proceed at a very rapid rate. However, the energy level diagram of ^{16}O shows that for temperatures up to about $T_9 \sim 2$, there is no level available in ^{16}O to foster a resonant reaction behavior. But since this nucleus is found in nature, its production must go through either: 1) a nonresonant direct capture reaction or 2) nonresonant captures into the tails of nearby resonances (subthreshold reactions).

Figure 12.10 shows, on the right of the ^{16}O energy levels, the threshold for the $^{12}\text{C} + {}^4\text{He}$ reaction, drawn at the appropriate level with respect to the ground state of the ^{16}O nucleus.

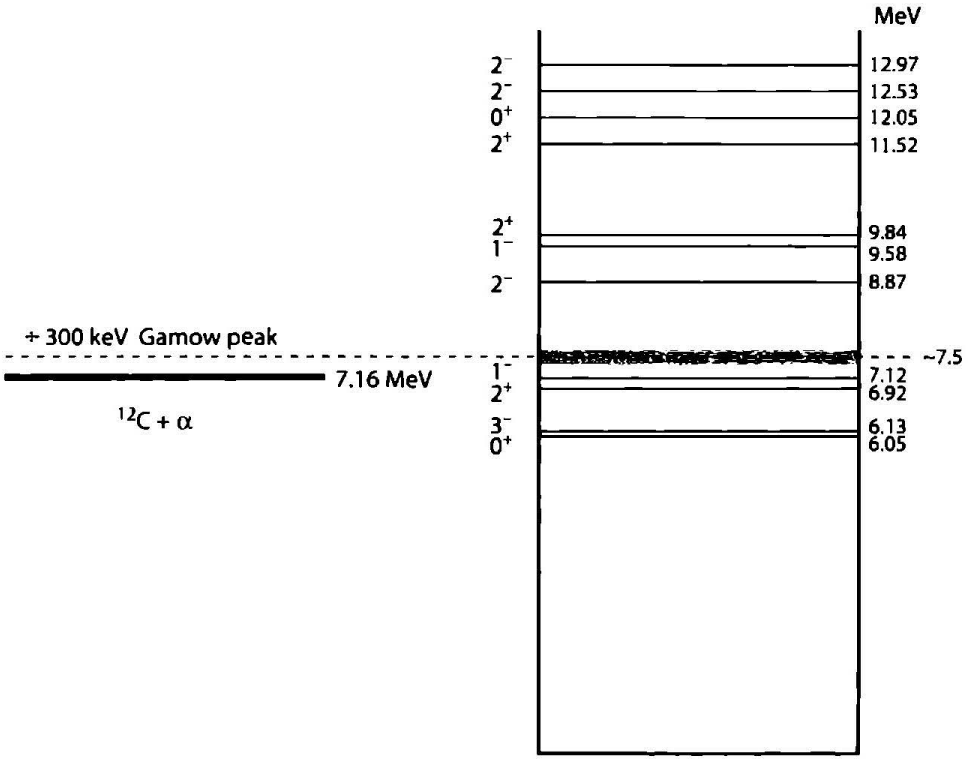

Figure 12.10 Energy levels of the ^{16}O nucleus near and above the α-particle threshold of capture on ^{12}C. The reaction rate is influenced mainly by the high energy tails of two subthreshold resonances in ^{16}O at $E_R = -45$ keV and $E_R = -245$ keV, plus the low energy tail of another high-lying broad resonance at 9580 keV.

The Gamow energy for temperatures $T_9 = 0.1$ and above indicates that for the expected central temperatures, the effective stellar (center of mass) energy region is near $E_0 = 0.3$ MeV. This energy region is reached by the low energy tail of a broad resonance centered at $E_{CM} = 2.42$ MeV above the threshold (the $J^\pi = 1^-$ state at 9.58 MeV above the ground state of ^{16}O) with a (relatively large) resonance width of 400 keV.

On the other hand, there are two subthreshold resonances in ^{16}O (at $E_X = 7.12$ MeV and $E_X = 6.92$ MeV), that is, -45 keV and -245 keV *below* the α-particle threshold that have $J^\pi = 1^-$ and $J^\pi = 2^+$, which contribute to the stellar burning rate by their high energy tails. However, electric dipole (E1) γ-decay of the 7.12 MeV state is inhibited by isospin selection rules. Had this not been the case, the $^{12}C(\alpha,\gamma)^{16}O$ reaction would have proceeded fast and ^{12}C would have been consumed during helium burning itself. The two subthreshold states at -45 keV and -245 keV give contributions to the astrophysical S factor of $S_{1^-}(E_0) = 0.1$ MeV barn and $S_{2^+}(E_0) = 0.2$ MeV barn, respectively, at the relevant stellar energy $E_0 = 0.3$ MeV. The state at $E_{CM} = 2.42$ MeV ($J^\pi = 1^-$ state at 9.58 MeV) gives a contribution $S_{1^-}(E_0) = 1.5 \times 10^{-3}$MeV barn. The total S-factor at $E_0 = 0.3$ MeV is therefore close to 0.3 MeV barn. These then provide low enough S or cross section not to burn the ^{12}C away entirely to ^{16}O, so that C/O $\sim$ 0.1 at the least.

Additionally, ^{16}O nuclei are not burned away by further α-capture in the reaction

A look at the level schemes of ^{20}Ne (see figure 12.11) shows the existence of an E_X = 4.97 MeV state ($J^\pi = 2^-$) in the Gamow window. However, this state cannot form in the resonance reaction due to considerations of parity conservation (unnatural parity of the resonant state). The lower 4.25 MeV state ($J^\pi = 4^+$) in ^{20}Ne also cannot act as a subthreshold resonance as it lies too far below threshold and is formed in the g-wave state. Therefore only direct capture reactions seem to be operative, which for (α, γ) reactions lead to cross sections in the range of nanobarns or below. Thus the destruction of the ^{16}O via $^{16}O(\alpha, \gamma)^{20}Ne$ reaction proceeds at a very slow rate during the stage of helium burning in red giant stars, for which the major ashes are carbon and oxygen.

To summarize, the synthesis of two important elements for the evolution of life as we know it on the earth depended on fortuitous circumstances of nuclear properties and selection rules for nuclear reactions. These are: 1) the mass of the unstable lowest (ground) state of ^{8}Be is close to the combined mass of two α-particles; 2) the resonance in ^{12}C at 7.65 MeV, enhances the α addition reaction (the second step); and 3) parity conservation has protected ^{16}O from being destroyed in the $^{16}O(\alpha, \gamma)^{20}Ne$ reactions by making the 4.97 MeV excited state in ^{20}Ne of unnatural parity.

12.9 Advanced Burning Stages

As helium burning progresses, the stellar core is increasingly made up of C and O. At the end of helium burning, all hydrogen and helium is converted into a mixture[2] of C and O, and since H, He are the most abundant elements in the original gas from which the star formed, the amounts of C and O are far more than the traces of heavy elements in the gas cloud.

Between these two products, the Coulomb barrier for further thermonuclear reaction involving the products is lower for C nuclei. At first the C + O rich core is surrounded by He burning shells and a helium rich layer, which in turn may be surrounded by a hydrogen burning shell and the unignited hydrogen rich envelope. When the helium burning ceases to provide sufficient power, the star begins to contract again under its own gravity and, as implied by the Virial theorem, the temperature of the helium exhausted core rises. The contraction continues until either the next nuclear fuel begins to burn at a rapid enough rate or electron degeneracy pressure halts the infall.

12.9.1 *Carbon burning*

Stars somewhat more massive than about 0.7 $M_\odot$ contract until the temperature is large enough for carbon to interact with itself (stars less massive may settle as degenerate helium *white dwarfs*). For stars more massive than $M \geq 8 - 10\ M_\odot$ (mass on the main sequence—*not* the mass of the C+O core), the contracting C+O core remains nondegenerate until C

[2] Note, however, the caveat: if the amount of ^{12}C is little due to a long stellar lifetime of He burning or to a larger rate of the $^{12}C + \alpha \rightarrow {}^{16}O + \gamma$ reaction whose estimate outlined in the earlier section is somewhat uncertain), then the star may directly go from the He burning stage to the O burning or Ne burning stage, skipping C burning altogether [Woo86].

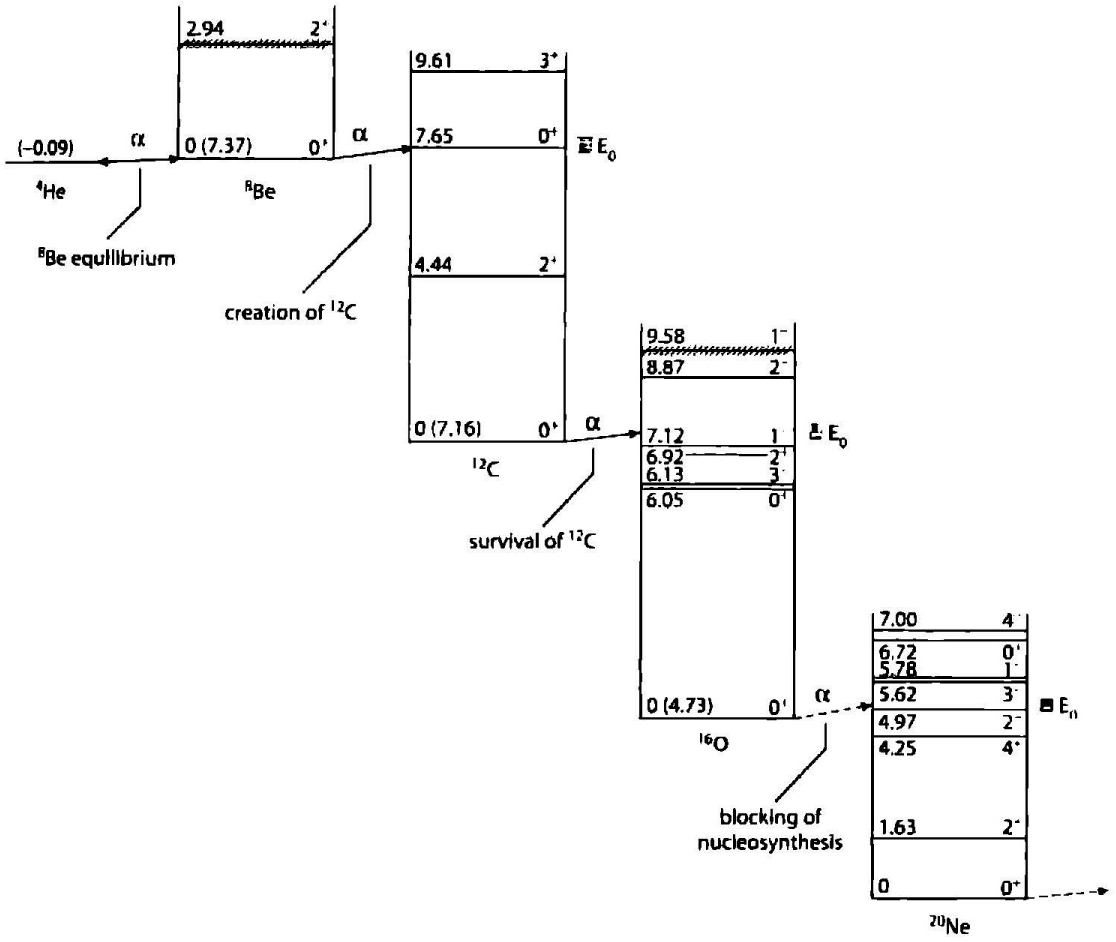

Figure 12.11 Energy levels of nuclei participating in thermonuclear reactions during the helium burning stage in red giant stars (adapted from [RR88]). The survival of both ^{12}C and ^{16}O in red giants, believed to be the source of terrestrial abundances depends upon fortuitous circumstances of nuclear level structures and other properties in these nuclei.

starts burning at $T \sim 5 \times 10^8 K$ and $\rho = 3 \times 10^6$ g cm^{-3}. Thereafter, sufficient power is generated and the contraction stops and quiescent (hydrostatic, not explosive) C burning proceeds.

The combined mass of two reacting ^{12}C nuclei falls at an excitation energy of 14 MeV in the compound nucleus of ^{24}Mg. At this energy there are many compound nuclear states, and the most effective range of stellar energies (the Gamow window) at the relevant temperature is about 1 MeV; hence a number of resonant states can contribute to the decay of the compound nucleus, and even the large angular momentum resonances may be important because the penetration factors in massive nuclei are not affected by centrifugal barriers. The carbon on carbon burning can proceed through multiple energetically allowed reaction channels:

$$^{12}C + {}^{12}C \rightarrow {}^{20}Ne + {}^{4}He \quad (Q = 4.62 \text{ MeV}) \tag{12.64}$$

$$\rightarrow {}^{23}Na + p \quad (Q = 2.24 \text{ MeV}) \tag{12.65}$$

$$\rightarrow {}^{23}Mg + n \quad (Q = -2.62 \text{ MeV}). \tag{12.66}$$

At the temperatures where carbon burning starts, the neutron liberating reactions require too much particle kinetic energy to be effective. In addition, based on laboratory measurements at higher energies compared to the stellar energies, the electromagnetic decay channel ($^{24}Mg + \gamma$) and the three-particle channel ($^{16}O + 2\alpha$) have lower probability compared to the two-particle channels $^{23}Na + p$ and $^{20}Ne + \alpha$. The latter two channels have nearly equal probabilities (see [Cla84]); at the lowest center of mass energies for which cross sections are measured in the laboratory for the proton and α channels (about 2.45 MeV), the branching ratios were $b_p \sim 0.6$ and $b_\alpha \sim 0.4$), and therefore the direct products of carbon burning are likely to be ^{23}Na, ^{20}Ne, protons, and α-particles. The rate for this reaction per pair of ^{12}C nuclei is [Ree59]

$$\log\lambda_{12,12} = \log f_{12,12} + 4.3 - \frac{36.55(1 + 0.1T_9)^{1/3}}{T_9^{1/3}} - \frac{2}{3}\log T_9, \tag{12.67}$$

where the factor $f_{12,12}$ is a screening factor. Now, at the temperatures of ^{12}C burning, the liberated protons and alpha particles can be quickly consumed through the reaction chain $^{12}C(p,\gamma)^{13}N(e^+\nu_e)^{13}C(\alpha,n)^{16}O$. Thus, the net effect is that the free proton is converted into a free neutron (which may be further captured) and the α-particle is consumed with ^{12}C into ^{16}O.

The α-particles are also captured by other α-particle nuclei, resulting in, at the end of carbon burning, nuclei like ^{16}O, ^{20}Ne, ^{24}Mg, and ^{28}Si. These secondary reactions augment the energy released by the initial carbon reaction, and Reeves [Ree59] estimated that each pair of ^{12}C nuclei releases about 13 MeV of energy. Toward the end of the carbon burning phase, other reactions such as $^{12}C+^{16}O$ and $^{12}C+^{20}Ne$ also take place. But these are less rapid and are not expected to play major roles compared to the $^{12}C+^{12}C$ reactions, due to their increased Coulomb barriers.

During the carbon burning and subsequent stages, the dominant energy loss from the star is due to neutrinos streaming out directly from the stellar thermonuclear furnace, rather than by photons from the surface. The neutrino luminosity is a sensitive function of core temperature and quickly outshines the surface photon luminosity of the star at the carbon burning stage. The (thermal) evolutionary timescale of the star, due to the neutrino emission, becomes very short and the core evolves rapidly—so rapidly (compared to the "cooling" timescale Kelvin-Helmholtz time $\tau_{KH} \sim GM^2/RL_{ph}$) that the conditions in the core are "not communicated" to the surface, since this communication happens by photon diffusion. The surface conditions (e.g., the temperature) of the star then do not markedly evolve as the core goes beyond the carbon burning stage, and it may not be possible just by looking at a star's surface conditions to understand whether the core is close to a supernova stage or has many thousands of years of hydrostatic thermonuclear burning to go.

12.9.2 Neon burning

The result of carbon burning is mainly neon, sodium, and magnesium, but aluminum and silicon are also produced in small quantities by the capture of α, p, and n released during carbon burning. When carbon fuel is exhausted, again the core contracts and its temperature T_c goes up. At approximately $T_9 \sim 1$, energetic photons from the high energy tail of

the Planck distribution function can begin to disintegrate the ^{20}Ne ash (see figure 12.11), so that one has the reaction $^{20}\text{Ne} + \gamma \rightarrow {}^{16}\text{O} + {}^{4}\text{He}$.

Nucleons in a nucleus are bound with typical binding energy of several to 8 MeV. An energetic γ-ray photon would be required to photo-eject a nucleon. Two-nucleon ejection would require more energy. Alpha-particles are, however, released at approximately the same energy as a nucleon due to the low separation energy of an α-particle in the nucleus. For example, the α separation energy in ^{20}Ne is 4.73 MeV. Thus, the major photonuclear reactions are (γ, n), (γ, p), and (γ, α) processes. For a photodisintegration reaction to proceed through an excited state E_X in the parent, the decay rate is

$$\lambda(\gamma, \alpha) = \left[\exp\left(-\frac{E_X}{kT}\right)\frac{2J_R + 1}{2J_0 + 1}\frac{\Gamma_\gamma}{\Gamma}\right] \times \frac{\Gamma_\alpha}{\hbar}. \tag{12.68}$$

In the above equation, the first factor in square brackets on the right-hand side is the probability of finding the nucleus in the excited state E_X and spin J_R (with J_0 being the ground state spin), while the second factor $\Gamma_\alpha/\hbar$ is the decay rate of the excited state with an α-particle emission. Now since $E_X = E_R + Q$, we have

$$\lambda(\gamma, \alpha) = \frac{\exp(-Q/kT)}{\hbar(2J_0 + 1)}(2J_R + 1)\frac{\Gamma_\alpha\Gamma_\gamma}{\Gamma}\exp\left(-\frac{E_R}{kT}\right). \tag{12.69}$$

At $T_9 \geq 1$, the photodisintegration is dominated by the 5.63 MeV level in ^{20}Ne (see figure 12.11). At approximately $T_9 \sim 1.5$, the photodissociation rate becomes greater than the rate for α capture on ^{16}O to produce ^{20}Ne (the reverse reaction), thus leading effectively to the net dissociation of ^{20}Ne. The released ^{4}He reacts with the unspent ^{20}Ne and leads to $^{4}\text{He} + {}^{20}\text{Ne} \rightarrow {}^{24}\text{Mg} + \gamma$. Thus the net result of the photodissociation of two ^{20}Ne nuclei is $2 \times {}^{20}\text{Ne} \rightarrow {}^{16}\text{O} + {}^{24}\text{Mg}$ with a net Q value of 4.58 MeV. The brief neon burning phase concludes at T_9 close to $\sim$1.

12.9.3 Oxygen burning

At the end of the neon burning the core is left with a mixture of α-particle nuclei ^{16}O and ^{24}Mg. After this another core contraction phase ensues and the core heats up, until at $T_9 \sim 2$, ^{16}O begins to react with itself,

$$^{16}\text{O} + {}^{16}\text{O} \rightarrow {}^{28}\text{Si} + {}^{4}\text{He} \tag{12.70}$$

$$\rightarrow {}^{32}\text{S} + \gamma. \tag{12.71}$$

The first reaction takes place approximately 45% of the time with a Q value of 9.593 MeV. In addition to Si and S, the O burning phase also produces Ar, Ca, and trace amounts of Cl, K, etc. up to Sc. Then at $T_9 \sim 3$, the produced ^{28}Si begins to burn in what is known as the Si burning phase.

12.9.4 Silicon burning

As we have seen, most of the stages of stellar helium burning involve thermonuclear fusion of nuclei to produce higher Z and A nuclei. The first exception is Neon burning, where

the photon field is sufficiently energetic to photodissociate neon before the temperature rises sufficiently to allow fusion reactions among oxygen nuclei to overcome their Coulomb repulsion. Processing in the neon burning phase takes place with the addition of helium nuclei to the undissociated neon rather than overcoming the Coulomb barrier of two neon nuclei. This trend continues in the silicon burning phase. In general, a photodisintegration channel becomes important when the temperature rises to the point that the Q-value, that is, the energy difference between the fuel and the products is smaller than approximately $30k_BT$.

With typical Q-values for reactions among stable nuclei above silicon being 8–12 MeV, photodisintegration of the nuclear products of neon and oxygen burning begins to play an important role once the temperature exceeds $T_9 \geq 3$. Then nuclei with smaller binding energies are destroyed by photodissociation in favor of their more tightly bound neighbors, and many nuclear reactions involving α-particles, protons, and neutrons interacting with all the nuclei in the mass range $A = 28$–65 take place. In contrast to the previous burning stages, where only a few nuclei underwent thermonuclear reactions among themselves, here the nuclear reactions are primarily of a rearrangement type, in which a particle is photoejected from one nucleus and captured by another and a given fuel nucleus is linked to a product nucleus by a multitude of reaction chains and cycles, so it is necessary to keep track of many more nuclei (and many reaction processes involving these) than for previous burning stages. More and more stable forms of the nuclei form in a nuclear reaction network as the rearrangement proceeds. Since there exists a maximum in the binding energy per nucleon at the ^{56}Fe nucleus, the rearrangements lead to nuclei in the vicinity of this nucleus (iron-group nuclei).

In the mass range $A = 28$–65, the levels in the compound nuclei that form in the reactions during silicon burning are so dense that they overlap. Moreover, at the high temperatures that are involved ($T_9 = 3$–5), the net reaction flux may be small compared to the large forward and backward reactions involving a particular nucleus and a quasi-equilibrium may ensue between groups of nuclei which are connected between separate groups by a few, slow, rate-limiting reactions ("bottlenecks"). However, as the available nuclear fuel(s) are consumed and thermal energy is removed due to escaping neutrinos, various nuclear reactions may no longer occur substantially rapidly ("freeze-out").

Weak interaction processes such as electron capture and β-decay of nuclei are important, by influencing the Y_e and thereby the reaction flow. These ultimately affect both the stellar core density and entropy structures, and it is important to track and include the changing Y_e (the number of electrons per nucleon) of the core material, not only in the silicon burning phase, but even from earlier oxygen burning phases.

For temperatures above 3×10^9 K, more photonuclear processes appear. These yield more nuclei to be burned and heavier nuclei are produced:

$$\gamma + {}^{28}_{14}\mathrm{Si} \rightarrow {}^{24}_{12}\mathrm{Mg} + {}^{4}_{2}\mathrm{He}, \quad {}^{4}_{2}\mathrm{He} + {}^{28}_{14}\mathrm{O} \rightarrow {}^{32}_{16}\mathrm{S} + \gamma, \text{ etc.} \tag{12.72}$$

Due to the large number of free neutrons, many (n,gamma) reactions (radiative neutron capture) elements in the mass range A=28-57 are formed. This leads to a large abundance

of elements in the iron mass region, which have the largest binding energy per nucleon. For elements heavier than iron the nuclear fusion processes do not generate energy.

For $A > 100$ the distribution of nuclei cannot be explained in terms of fusion reactions with charged particles. They are formed by the successive capture of slow neutrons and of β^- decay. The maxima of the element distribution in $N = 50, 82, 126$ are due to the small capture cross sections corresponding to the magic numbers. This yields a trash of isotopes at the observed element distribution.

12.10 Synthesis of Heaviest Elements

So far we have been dealing primarily with charged particle reactions and photodisintegration which lead to the production of lighter elements ($A = 1$–40) and the recombination reactions for the production of elements, $A = 40$–65. However, the heavier elements ($A \geq 65$), because of their high charge and relatively weak stability, cannot be produced by these two processes. It was therefore natural to investigate the hypothesis of neutron-induced reactions on the elements that are formed already in the various thermonuclear burning stages, and in particular on the iron group elements.

The study of the nuclear reaction chains in stellar evolution shows that during certain phases large neutron fluxes are released in the core of a star. On the other hand, the analysis of the relative abundance of elements shows certain patterns that can be explained in terms of the neutron absorption cross sections of these elements. If the heavier elements above the iron peak were to be synthesized during, for example, charged particle thermonuclear reactions during silicon burning, their abundance would drop much more steeply with increasing mass (larger and larger Coulomb barriers) than the observed behavior of abundance curves, which shows a much lesser than expected decrease. Based on the abundance data, Suess and Urey [Sue56] and Burbidge et al. [Bur57] (hereafter B^2FH) argued that heavy elements are made instead by thermal neutron capture.

Two distinct neutron processes are required to make the heavier elements. The slow neutron capture process (s process) has a lifetime for β-decay τ_β shorter than the competing neutron capture time τ_n ($\tau_\beta \leq \tau_n$). This makes the s process nucleosynthesis run through the valley of β-stability. The rapid neutron capture r process, on the other hand, requires $\tau_n \ll \tau_\beta$. This process takes place in extremely neutron rich environments, for the neutron capture timescale is inversely proportional to the ambient neutron density. The r process, in contrast to the s process, goes through very neutron rich and unstable nuclei that are far off the valley of stability. The relevant properties of such nuclei are most often not known experimentally, and are usually estimated theoretically. Some of the key parameters are the half-lives of the β-unstable nuclei along the s process path. But the nuclear half-life in the stellar environment can change not just due to transitions from the ground state of the parent nucleus, but also because its excited states are thermally populated.

In the r process, the β-decay properties of the nuclei regulate the reaction flow to larger charge numbers and determine the resultant abundance pattern and the duration of the process. The r process lasts for typically a few seconds, in an intense neutron density

environment $n_n \sim 10^{20}$–10^{25}cm^{-3}. In comparison, the neutron densities in the s process are much more modest, say $n_n \sim 10^8\text{cm}^{-3}$; these neutron irradiation can take place, for example, in the helium burning phase of red giant stars. Nuclei above the iron group up to about $A = 90$ are produced in massive stars mainly by the s process. Above $A = 100$ the s process does very little in massive stars, although there are redistributions of some of the heavy nuclei. Most of the s process above mass 90 is believed to come from asymptotic giant branch (AGB) stars.

12.11 White Dwarfs and Neutron Stars

If the thermonuclear processes in massive stars achieve the production of iron, there are the following possibilities for the star evolution.

(a) For stars with masses $<1.2\ M_\odot$ the internal pressure of the degenerated electron gas (when the electrons occupy all states allowed by the Pauli principle) does not allow star compression due to the gravitational attraction continuing indefinitely. For a free electron gas at temperature $T = 0$ (lowest energy state), the electrons occupy all energy states up to the Fermi energy. The total density of the star can be calculated by adding up the individual electronic energies. Since each phase-space cell $d^3p \cdot V$ (where V is the volume occupied by the electrons) contains $d^3p \cdot V/(2\pi\hbar)^3$ states, we get

$$\frac{E}{V} = 2\int_0^{p_i} \frac{d^3p}{(2\pi\hbar)^3}\, E(p) = 2\int_0^{p_F} \frac{d^3p}{(2\pi\hbar)^3}\sqrt{p^2c^2 + m_e^2c^4} = n_0 m_e c^2 x^3 \epsilon(x),$$

$$\epsilon(x) = \frac{3}{8x^3}\left\{x(1+2x^2)(1+x^2)^{1/2} - \log|x + (1+x)^{1/2}|\right\}, \tag{12.73}$$

where the factor 2 is due to the electron spin, and

$$x = \frac{p_F c}{m_e c^2} = \left(\frac{n}{n_0}\right)^{1/3} = \left(\frac{\rho}{\rho_0}\right)^{1/3}, \tag{12.74}$$

where

$$n_0 = \frac{me^3c^1}{h^3} \quad \text{and} \quad \rho_0 = \frac{m_N n_0}{Y_e} = 9.79 \times 10^5\ Y_e^{-1}\ \text{g/cm}^3. \tag{12.75}$$

In the above relations p_F is the Fermi momentum of the electrons, m_e (m_N) is the electron (nucleon) mass, n is the density of electrons, and ρ is the mass density in the star. Y_e is the number of electrons per nucleon.

The variable x characterizes the electron density in terms of

$$n_0 = 5.89 \times 10^{29}\ \text{cm}^{-3}. \tag{12.76}$$

At this density the Fermi momentum is equal to the inverse of the Compton wavelength of the electron.

Using traditional methods of thermodynamics, the pressure is related to the energy variation by

$$P = -\frac{\partial E}{\partial V} = -\frac{\partial E}{\partial x}\frac{\partial x}{\partial V} = -\frac{\partial E}{\partial x}\left(-\frac{x}{3V}\right) = \frac{1}{3}\, n_0 m_e c^2 x^4 \frac{d\epsilon}{dx}. \tag{12.77}$$

This model allows us to calculate the pressure in the electron gas in a very simple form. Since the pressure increases with the electron density, which increases with the decreasing volume of the star, we expect that the gravitational collapse stops when the electronic pressure equals the gravitational pressure. When this occurs the star cools slowly and its luminosity decreases. The star becomes a *white dwarf* and in some cases its diameter can become smaller than that of the moon.

(b) For stars with masses in the interval 1.2–1.6 $M_\odot$, the electron pressure is not sufficient to balance the gravitational attraction. The density increases to 2×10^{14} g cm^{-3} and the matter "neutronizes." This occurs via electron capture by the nuclei (inverse beta decay), transforming protons into neutrons. The final product is a *neutron star*, with a small radius (see figure 12.12). For example, if it were possible to form a neutron star from the sun it would have a radius given by

$$\left(\frac{M_\odot}{\frac{4\pi}{3}\rho}\right)^{1/3} = \left(\frac{2 \times 10^{33}\,\text{g}}{\frac{4\pi}{3} \times 2 \times 10^{14}\,\text{g cm}^{-3}}\right)^{1/3} \simeq 14\ \text{km}.$$

The process of transformation of iron nuclei into neutron matter occurs as follows. For densities of the order of 1.15×10^9 g cm^{-3} the Fermi energy of the electron gas is larger than the upper energy of the energy spectrum for the β-decay of the isotope $^{56}_{25}$Mn. The decay of this isotope can be inverted and two neutron rich isotopes of $^{56}_{25}$Mn are formed, that is,

$$^{56}_{26}\text{Fe} + \text{e}^- \rightarrow {}^{56}_{25}\text{Mn} + \nu_e\,. \tag{12.78}$$

These nuclei transform in $^{56}_{24}$Cr by means of the reaction

$$^{56}_{25}\text{Mn} + \text{e}^- \rightarrow {}^{56}_{24}\text{Cr} + \nu_e. \tag{12.79}$$

With the increasing of the pressure more isotopes can be formed, until neutrons start being emitted

$$^{A}_{Z}\text{X} + \text{e}^- \rightarrow {}^{A}_{Z-1}\text{X} + \text{n} + \nu_e. \tag{12.80}$$

For $^{56}_{26}$Fe this reaction network starts to occur at an energy of 22 MeV, which corresponds to a density of 4×10^{11} g cm^{-3}. With increasing density, the number of free neutrons increases and, when the density reaches 2×10^{14} g cm^{-3}, the density of free neutrons is 100 times larger than the density of the remaining electrons.

A *pulsar* is a rapidly rotating neutron star. Like a black hole, it is an endpoint to stellar evolution. The "pulses" of high energy radiation we see from a pulsar are due to a misalignment of the neutron star's rotation axis and its magnetic poles (see figure 12.13). Neutron stars for which we see such pulses are called "pulsars." They have a mass 40% larger than the sun and their radius is just 20 kilometers. This means that a cubic centimeter of this matter weighs 100 million tons! The neutron stars are at the limit of density that matter can have, the subsequent step being a black hole. Today we know more than 600 pulsars, and they are formidable astrophysics laboratories, since (a) their density is comparable to that of an atomic nucleus; (b) their mass and size give place to gravitational fields smaller than those of the black holes, but easier to measure; (c) the fastest of the pulsars has 600 turns about its axis in one second, so, its surface rotates at 36,000 kilometers a second;

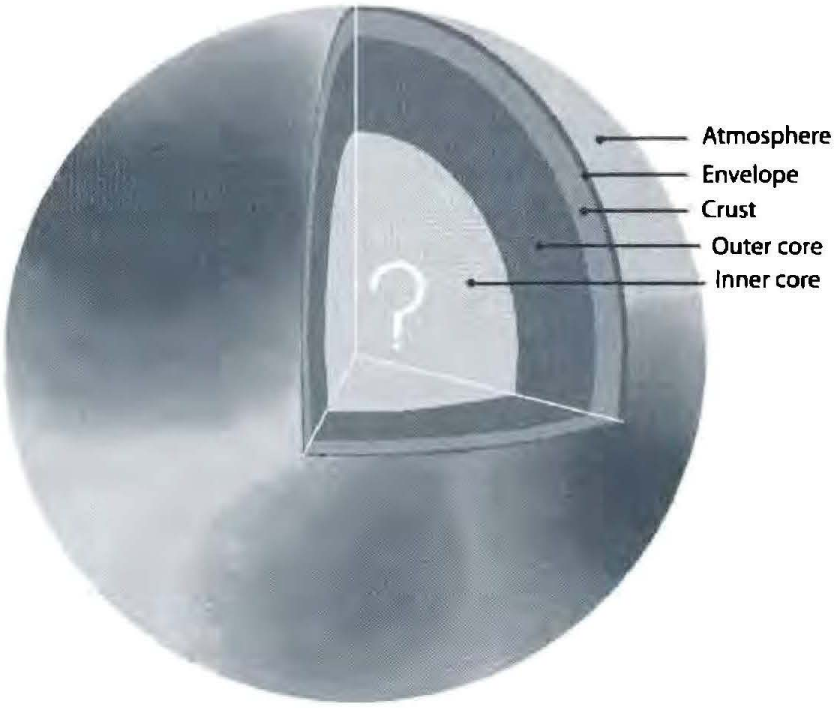

Figure 12.12 The structure of a neutron star. The outer regions of a neutron star may consist of thin layers of various elements that were produced by nuclear reactions during the star's lifetime. These outer layers are thought to have a rigid crystalline structure because of the intense gravitational field of the neutron star. The composition of the inner core is unknown.

(d) neutron stars have more intense magnetic fields than any other known object in the universe, million of times stronger than those produced in any terrestrial laboratory; (e) in some cases the regularity of their pulsations is the same or greater than the precision of the atomic clock, the latter being otherwise the best we have.

Figure 12.14 shows the relative distribution of elements in our galaxy. It has two distinct regions: in the region $A < 100$ it decreases with A approximately like an exponential, whereas for $A > 100$ it is approximately constant, except for the peaks in the region of the magic numbers $Z = 50$ and $N = 50, 82, 126$.

12.12 Supernova Explosions

It has long been observed that, occasionally, a new star appears in the sky, increases in brightness to a maximum value, and decays afterward until its visual disappearance. Such stars were called *novae*. Among the novae some stars present an exceptional variation in brightness and are called *supernovae*.

Schematically a pre-supernova has the onion structure presented in figure 12.15. Starting from the center of the star, we first find a core of iron, the remnant of silicon burning. After that we pass successive regions where ^{28}Si, ^{16}O, ^{12}C, ^{4}He, and ^{1}H form the dominant fraction. In the interfaces, nuclear burning continues to happen.

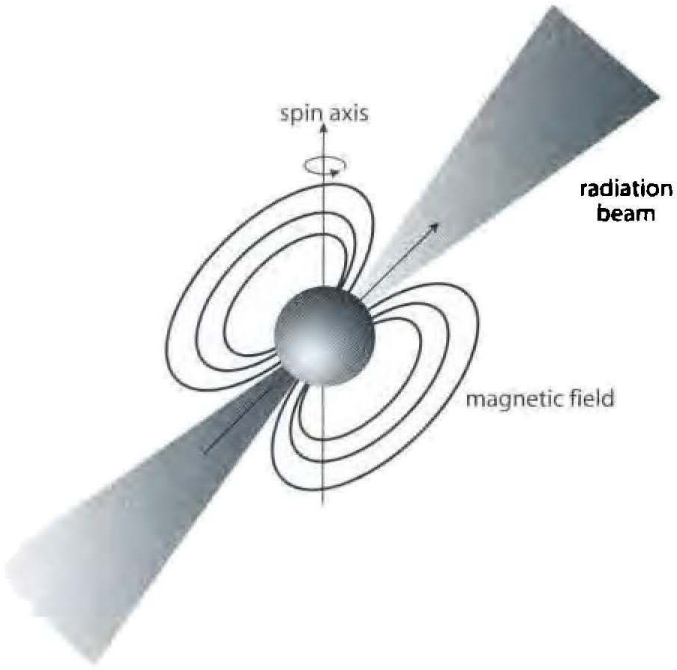

Figure 12.13 A rapidly rotating neutron star, or pulsar. At the magnetic poles, particles can escape and give rise to radio emission. If the magnetic axis is misaligned with the rotation axis of the neutron star (as shown), the star's rotation sweeps the beams over the observer as it rotates like a lighthouse, and one sees regular, sharp pulses of light (optical, radio, X-ray, etc.).

Silicon burning exhausts the nuclear fuel. As we mentioned previously, the gravitational collapse of the iron core cannot be held by means of pressure heat from nuclear reactions. However, Chandrasekhar [Ch31] showed that a total collapse can be avoided by electronic pressure. In this situation, the core is stabilized due to the pressure of the degenerated electron gas, $P(r)$, and the inward gravitational pressure. This means that for a given point inside the star,

$$
\begin{aligned}
-\frac{Gm(r)}{r^2}\,\rho(r) &= \frac{dP(r)}{dr} = \frac{d\rho}{dr}\,\frac{dP}{d\rho}, \\
\frac{dm}{dr} &= 4\pi r^2 \rho(r), \\
\frac{dP}{d\rho} &= Y_e\,\frac{m_e}{m_N}\,\frac{x^2}{3\sqrt{1+x^2}}.
\end{aligned}
\tag{12.81}
$$

where x and Y_e are defined following (12.73).

This model is appropriate for a nonrotating white dwarf. With the boundary conditions $m(r=0)=0$ and $\rho(r=0)=\rho_c$ (the central density), these equations can be solved easily [Ko86]. For a given Y_e, the model is totally determined by ρ_c. Figure 12.16 shows the mass density of a white dwarf. We observe that the total mass of a white dwarf (of the order of a solar mass, $M_\odot = 1.98 \times 10^{33}$ g) increases with ρ_c. Nonetheless, and perhaps most important, it cannot exceed the finite value of

M </= Mch = 1.45(2Ye)^2 M_sun 12.82

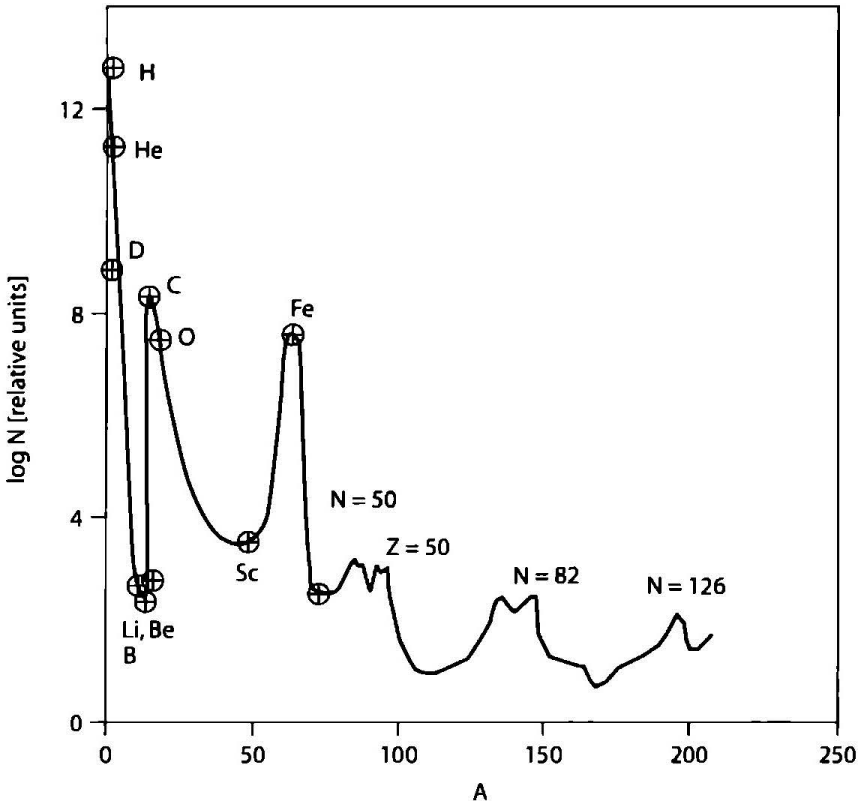

Figure 12.14 Relative distribution of elements in our galaxy.

known as the *Chandrasekhar mass* [Ch31]. Applying these results to the nucleus of a star with any mass, we get from (12.81) that stars with mass $M > M_{Ch}$ cannot be stable against gravitational collapse by the pressure of the degenerate electron gas. The collapse occurs inevitably for a massive star, since the silicon burning adds more and more material to the stellar core.

At the beginning of the collapse the temperature and density are of the order of $T \sim 10^{10}$ K and $\rho \sim 3 \times 10^9$ g/cm^3. The core is made of ^{56}Fe and of electrons. There are two possibilities, both accelerating the collapse.

1. At conditions present in the collapse the strong reactions and the electromagnetic reactions between the nuclei are in inverse equilibrium,

$$\gamma + {}^{56}_{26}\mathrm{Fe} \Longleftrightarrow 13({}^4\mathrm{He}) + 4n - 124\ \mathrm{MeV}. \tag{12.83}$$

For example, with $\rho = 3 \times 10^9$ g/cm^3 and $T = 11 \times 10^9$ K, half of ^{56}Fe is dissociated. This dissociation takes energy from the core and causes pressure loss. The collapse is thus accelerated.

2. If the mass of the core exceeds M_{Ch}, electrons are captured by the nuclei to avoid violation of the Pauli principle

$$e^- + (Z, A) \rightarrow (Z - 1, A) + \nu_e. \tag{12.84}$$

The neutrinos can escape the core, taking away energy. This is again accompanied by a pressure loss due to the decrease of the free electrons (this also decreases M_{Ch}). The collapse is again accelerated.

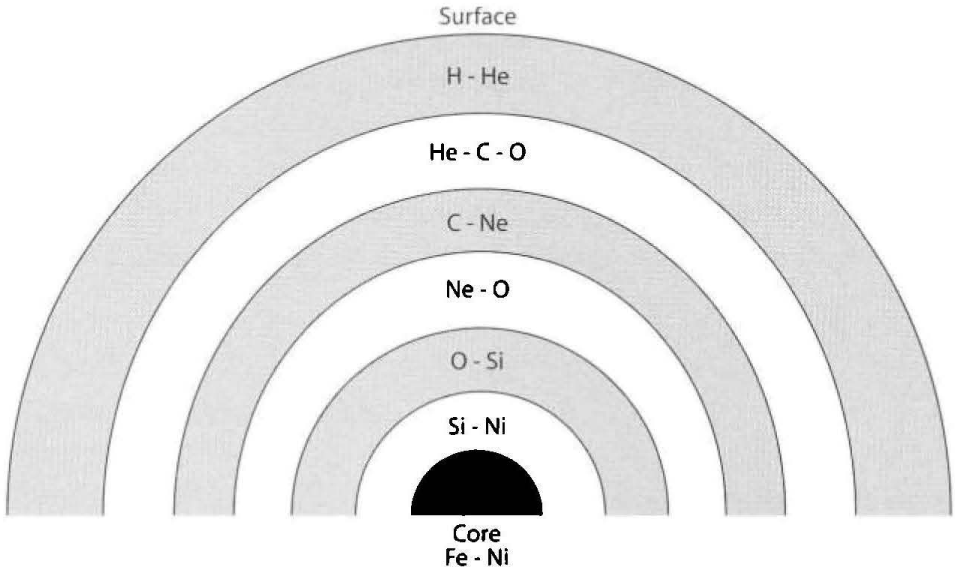

Figure 12.15 The "onion" structure of a $20M_{\odot}$ star just before a supernova explosion.

The gravitational contraction increases the temperature and density of the core. An important change in the physics of the collapse occurs when the density reaches $\rho_{\text{trap}} \simeq 4 \times 10^{11}$ g/cm^3. The neutrinos become essentially confined to the core, since their diffusion time in the core is larger than the collapse time. After the neutrino confinement no energy is taken out of the core. Also, all reactions are in equilibrium, including the capture process (12.84). The degeneracy of the neutrino Fermi gas avoids a complete neutronization, directing the reaction (12.84) to the left. As a consequence, Y_e remains large during the collapse ($Y_e \approx 0.3$–0.4 [Be79]). To equilibrate the charge, the number of protons must also be large. To reach $Z/A = Y_e \approx 0.3$–0.4, the protons must be inside heavy nuclei that will therefore survive the collapse.

Two consequences follow

1. The pressure is given by the degenerate electron gas that controls the whole collapse; the collapse is thus adiabatic, with the important consequence that the collapse of the most internal part of the core is *homologous*, that is, the position $r(t)$ and the velocity $v(t)$ of a given element of mass of the core are related by

$$r(t) = \alpha(t) r_0; \quad v(t) = \frac{\dot{\alpha}}{\alpha} r(t), \tag{12.85}$$

where r_0 is the initial position.

2. Since the nuclei remain in the core of the star, the collapse has a reasonably large order and the entropy remains small during the collapse [Be79] ($S \approx 1.5\, k$ per nucleon, where k is the Boltzmann constant).

The collapse continues homologously until nuclear densities of the order of $\rho_N \approx 10^{14}$ g/cm^3 are reached, when the matter can be thought as approximately a degenerate Fermi gas of nucleons. Since the nuclear matter has a finite compressibility, the homologous core decelerates and starts to increase again as a response to the increase of the nuclear

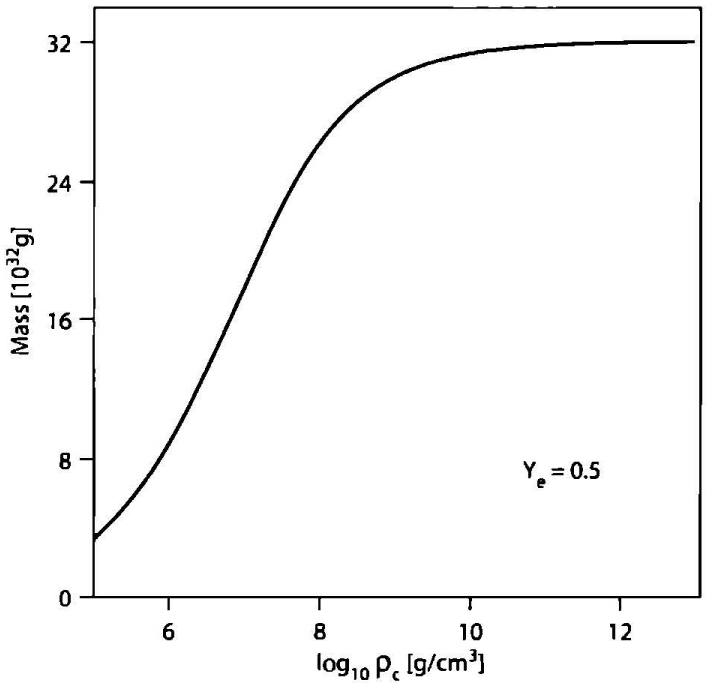

Figure 12.16 Masses of white dwarfs calculated as a function of ρ_c, the central density. With increasing ρ_c, the mass reaches a limiting value, the Chandrasekhar mass.

matter. This eventually leads to a *shock wave* which propagates to the external core (the iron core outside the homologous core), which, during the collapse time, continues to contract reaching the supersonic velocity. The collapse break followed by the shock wave is the mechanism which creates the supernova explosion. Nonetheless, several ingredients of this scenario are still unknown, including the equation of state of the nuclear matter. The compressibility influences the available energy for the shock wave, which must be of the order of 10^{51} erg.

The exact mechanism for the explosion of a supernova is still controversial.

1. In the *direct mechanism*, the shock wave is not only strong enough to stop the collapse, but also to explode the exterior stellar shells.

2. If the energy in the shock wave is insufficient for a direct explosion, the wave will deposit its energy in the exterior of the core, e.g., by excitation of the nuclei, being frequently followed by electronic capture and emission of neutrinos (*neutrino eruption*). Additionally, neutrinos of the all three species are generated by the production of pairs in the hot environment. A new shock wave can be generated by the outward diffusion of neutrinos, indeed carrying the most part of the energy liberated in the gravitational collapse of the core ($\approx 10^{53}$ erg). If about 1% of the energy of the neutrinos is converted into kinetic energy due to the coherent neutrino-nucleus scattering, a new shock wave arises. This will be strong enough to explode the star. This process is known as the *retarded mechanism* for supernova explosion.

To know which of the above mechanism is responsible for the supernova explosion, one needs to know the rate of electron capture, the nuclear compressibility, and the way

neutrinos are transported. The iron core, the remnant of the explosion (the homologous core and part of the external core) will not explode and will become either a neutron star, and possibly later a *pulsar* (rotating neutron star), or a *black hole*, as in the case of more massive stars, with $M \geq 25\text{–}35 M_{\odot}$.

Type II supernovae are defined as those showing H-lines in their spectra. It is likely that most, if not all, of the exploding massive stars still have some H-envelope left, and thus exhibit such a feature. In contrast, Type I supernovae lack H in their ejecta.

12.13 Nuclear Reaction Models

Explosive nuclear burning in astrophysical environments produces unstable nuclei, which again can be targets for subsequent reactions. In addition, it involves a very large number of stable nuclei, which are not fully explored by experiments. Thus, it is necessary to be able to predict reaction cross sections and thermonuclear rates with the aid of theoretical models. Especially during the hydrostatic burning stages of stars, charged particle induced reactions proceed at such low energies that a direct cross section measurement is often not possible with existing techniques. Hence extrapolations down to the stellar energies of the cross sections measured at the lowest possible energies in the laboratory are the usual procedures to apply. To be trustworthy, such extrapolations should have as strong a theoretical foundation as possible. Theory is even more mandatory when excited nuclei are involved in the entrance channel, or when unstable very neutron rich or neutron deficient nuclides (many of them being even impossible to produce with present-day experimental techniques) have to be considered. Such situations are often encountered in the modeling of explosive astrophysical scenarios.

Various models have been developed in order to complement the experimental information.

12.13.1 *Microscopic models*

In this model, the nucleons are grouped into clusters, as was explained in section 3.12. Keeping the internal cluster degrees of freedom fixed, the totally antisymmetrized relative wavefunctions between the various clusters are determined by solving the Schrödinger equation for a many-body Hamiltonian with an effective nucleon-nucleon interaction. When compared with most others, this approach has the major advantage of providing a consistent, unified and successful description of the bound, resonant, and scattering states of a nuclear system. Various improvements of the model have been made [Des98].

The microscopic model has been applied to many important reactions involving light systems, and in particular to the various p-p chain reactions [Lan96]. The available experimental data can generally be well reproduced. The microscopic cluster model (or its variant, the microscopic potential model) has also made an important contribution to the understanding of the key $^{12}C(\alpha, \gamma)^{16}O$ reaction rate [Des93a].

12.13.2 Potential and DWBA models

The potential model has been known for a long time to be a useful tool in the description of radiative capture reactions. It assumes that the physically important degrees of freedom are the relative motion between the (structureless) nuclei in the entrance and exit channels, and by the introduction of spectroscopic factors and strength factors in the optical potential. The associated drawbacks are that the nucleus-nucleus potentials adopted for calculating the initial and final wavefunctions from the Schrödinger equation cannot be unambiguously defined, and that the spectroscopic factors cannot be derived from first principles. They have instead to be obtained from more or less rough "educated guesses."

In the *potential model* the bound state wavefunctions of $c = a + b$ are specified by

$$\Psi_{JM}(\mathbf{r}) = \frac{u^J_{lj}(r)}{r}\mathcal{Y}^l_{JM}\,. \tag{12.86}$$

where $\mathbf{r}$ is the relative coordinate of a and b, $u^J_{lj}(r)$ is the radial wavefunction and $\mathcal{Y}^l_{JM}$ is the spin-angle wavefunction

$$\mathcal{Y}^l_{JM} = \sum_{m_l M_a} \left(jmI_aM_a|JM\right)|jm\rangle|I_aM_a\rangle\,, \quad \text{with} \quad |jm\rangle = \sum_{m_l,\,M_b} Y_{lm_l}(\hat{\mathbf{r}})\chi_{M_b}, \tag{12.87}$$

where χ_{M_b} is the spinor wavefunction of particle b and $\left(jmI_aM_a|JM\right)$ is a Clebsch-Gordan coefficient.

As described in chapter 9, the operators for electric transitions of multipolarity $\lambda\pi$ are given by

$$\mathcal{M}_{E\lambda\mu} = e_\lambda\, r^\lambda Y_{\lambda\mu}(\hat{\mathbf{r}}), \tag{12.88}$$

where the effective charge, which takes into account the displacement of the center of mass, is

$$e_\lambda = Z_b e\left(-\frac{m_a}{m_c}\right)^\lambda + Z_a e\left(\frac{m_b}{m_c}\right)^\lambda. \tag{12.89}$$

For magnetic dipole transitions,

$$\mathcal{M}_{M1\mu} = \sqrt{\frac{3}{4\pi}}\mu_N\left[e_M l_\mu + \sum_{i=a,b} g_i(s_i)_\mu\right], \quad e_M = \left(\frac{m_a^2 Z_a}{m_c^2} + \frac{m_b^2 Z_b}{m_c^2}\right), \tag{12.90}$$

where l_μ and s_μ are the spherical components of order μ ($\mu = -1, 0, 1$) of the orbital and spin angular momentum ($\mathbf{l} = -i\mathbf{r}\times\nabla$, and $\mathbf{s} = \boldsymbol{\sigma}/2$) and g_i are the gyromagnetic factors of particles a and b. The nuclear magneton is given by $\mu_N = e\hbar/2m_Nc$.

The matrix element for the transition $J_0M_0 \to JM$, using the convention of [BM69] is given by reduced matrix element and a Clebsch due to Wigner-Eckart theorem.

The multipole strength, or response function, for a particular partial wave, summed over final channel spins, is defined by

$$\frac{dB(\pi\lambda;\, l_0 j_0 \to klj)}{dk} = \sum_J \frac{|\langle kJ \,\|\mathcal{M}_{\pi\lambda}\| J_0\rangle|^2}{2J_0+1}, \tag{12.92}$$

where $\pi = E$, or M. In this equation $l_0 j_0$ (lj) are the ground (continuum) state angular momentum quantum numbers and k denotes the relative momentum of the final (continuum) state (the relative energy is $E = \hbar^2 k^2/2\mu$, where μ is the reduced mass of a + b).

The photo-absorption cross section for the reaction $\gamma + c \to a + b$ is given in terms of the response function by

$$\sigma_\gamma^{(\lambda)}(E_\gamma) = \frac{(2\pi)^3(\lambda+1)}{\lambda\left[(2\lambda+1)!!\right]^2}\left(\frac{m_{ab}}{\hbar^2 k}\right)\left(\frac{E_\gamma}{\hbar c}\right)^{2\lambda-1}\frac{dB(\pi\lambda)}{dE}, \tag{12.93}$$

where $E_\gamma = E + |E_B|$, with $|E_B|$ being the binding energy of the $a + b$ system.

The cross section for the radiative capture process $a + b \to c + \gamma$ can be related by detailed balance to (12.93), that is,

$$\sigma_{(\pi\lambda)}^{(\mathrm{rc})}(E) = \left(\frac{E_\gamma}{\hbar c}\right)^{2\lambda-1}\frac{2(2I_c+1)}{(2I_a+1)(2I_b+1)}\sigma_\gamma^{(\lambda)}(E_\gamma). \tag{12.94}$$

The total capture cross section σ_{nr} is determined by the capture to all bound states with the single particle spectroscopic factors S_i in the final nucleus

$$\sigma_{\mathrm{nr}}(E) = \sum_{i,\pi,\lambda} S_i\, \sigma_{(\pi\lambda),i}^{(\mathrm{rc})}(E). \tag{12.95}$$

Experimental information or detailed shell model calculations have to be performed to obtain the spectroscopic factors S_i.

12.13.3 Parameter fit

Reaction rates dominated by the contributions from a few resonant or bound states are often extrapolated in terms of *R- or K-matrix* fits, which rely on quite similar strategies. A sketch of *R*-matrix theory was presented in section 4.9. The appeal of these methods rests on the fact that analytical expressions which allow for a rather simple parametrization of the data can be derived from underlying formal reaction theories. However, the link between the parameters of the *R*-matrix model and the experimental data (resonance energies and widths) is only quite indirect. The *K*-matrix formalism solves this problem, but suffers from other drawbacks [Bar94].

The *R*- and *K*-matrix models have been applied to a variety of reactions, in particular to the analysis of the $^{12}C(\alpha,\gamma)^{16}O$ reaction rate [Az95].

12.13.4 Statistical models

Many astrophysical scenarios involve a wealth of reactions on intermediate mass or heavy nuclei. This concerns the nonexposive or explosive burning of C, Ne, O and Si, as well

as the s-, r- and p-process nucleosynthesis. Fortunately, a large fraction of the reactions of interest proceed through compound systems that exhibit high enough level densities for statistical methods to provide a reliable description of the reaction mechanism. In this respect, the *Hauser-Feshbach (HF) model* has been widely used with considerable success. Explosive burning in supernovae involves in general intermediate mass and heavy nuclei. Due to a large nucleon number, they have an intrinsically high density of excited states. A high density in the compound nucleus at the appropriate excitation energy allows one to make use of the statistical model approach for compound nuclear reactions [HF52] which averages over resonances. Averaged transmission coefficients T, which do not reflect a resonance behavior, but rather describe absorption via an imaginary part in the (optical) nucleon-nucleus potential as described in [MW79]. This leads to the expression derived in section 4.14,

$$\sigma_i^{\mu\nu}(j,o;E_{ij}) = \frac{\pi\hbar^2/(2\mu_{ij}E_{ij})}{(2J_i^\mu+1)(2J_j+1)} \times \sum_{J,\pi}(2J+1)\frac{T_j^\mu(E,J,\pi,E_i^\mu,J_i^\mu,\pi_i^\mu)T_o^\nu(E,J,\pi,E_m^\nu,J_m^\nu,\pi_m^\nu)}{T_{\text{tot}}(E,J,\pi)} \tag{12.96}$$

for the reaction $i^\mu(j,o)m^\nu$ from the target state i^μ to the excited state m^ν of the final nucleus, with a center of mass energy E_{ij} and reduced mass μ_{ij}. J denotes the spin, E the corresponding excitation energy in the compound nucleus, and π the parity of excited states. When these properties are used without subscripts they describe the compound nucleus, while subscripts refer to states of the participating nuclei in the reaction $i^\mu(j,o)m^\nu$ and superscripts indicate the specific excited states. Experiments measure $\sum_\nu \sigma_i^{0\nu}(j,o;E_{ij})$, summed over all excited states of the final nucleus, with the target in the ground state. Target states μ in an astrophysical plasma are thermally populated and the astrophysical cross section $\sigma_i^*(j,o)$ is given by

$$\sigma_i^*(j,o;E_{ij}) = \frac{\sum_\mu (2J_i^\mu+1)\exp(-E_i^\mu/kT)\sum_\nu \sigma_i^{\mu\nu}(j,o;E_{ij})}{\sum_\mu (2J_i^\mu+1)\exp(-E_i^\mu/kT)}. \tag{12.97}$$

The summation over ν replaces $T_o^\nu(E,J,\pi)$ in (12.96) by the total transmission coefficient

$$T_o(E,J,\pi) = \sum_{\nu=0}^{\nu_m} T_o^\nu(E,J,\pi,E_m^\nu,J_m^\nu,\pi_m^\nu) + \int_{E_m^{\nu_m}}^{E-S_{m,o}} \sum_{J_m,\pi_m} T_o(E,J,\pi,E_m,J_m,\pi_m)\rho(E_m,J_m,\pi_m)dE_m. \tag{12.98}$$

Here $S_{m,o}$ is the channel separation energy, and the summation over excited states above the highest experimentally known state ν_m is changed to an integration over the level density ρ. The summation over target states μ in (12.97) has to be generalized accordingly.

The important ingredients of statistical model calculations as indicated in the above equations are the particle and γ transmission coefficients T and the level density of excited states ρ. Therefore, the reliability of such calculations is determined by the accuracy with which these components can be evaluated (often for unstable nuclei).

The gamma transmission coefficients have to include the dominant gamma transitions (E1 and M1) in the calculation of the total photon width. The smaller, and therefore less important, M1 transitions have usually been treated with the simple single particle approach $T \propto E^3$ of [BW52]. The E1 transitions are usually calculated on the basis of the Lorentzian representation of the giant dipole resonance (see section 6.8). Within this model, the E1 transmission coefficient for the transition emitting a photon of energy E_γ in a nucleus ${}^{A}_{N}Z$ is given by

$$T_{E1}(E_\gamma) = \frac{8}{3}\frac{NZ}{A}\frac{e^2}{\hbar c}\frac{1+\chi}{mc^2}\sum_{i=1}^{2}\frac{i}{3}\frac{\Gamma_{G,i}E_\gamma^4}{(E_\gamma^2 - E_{G,i}^2)^2 + \Gamma_{G,i}^2 E_\gamma^2}. \tag{12.99}$$

Here $\chi\,(=0.2)$ accounts for the neutron-proton exchange contribution, and the summation over i includes two terms that correspond to the split of the GDR in statically deformed nuclei, with oscillations along ($i = 1$) and perpendicular ($i = 2$) to the axis of rotational symmetry.

12.14 Exercises

1. (a) What is the most probable kinetic energy of a hydrogen atom at the interior of the sun ($T = 1.5 \times 10^7$ K)? (b) What fraction of these particles would have kinetic energy in excess of 100 keV?

2. Suppose the iron core of a supernova star has a mass of 1.4 $M_\odot$ (the sun's mass is $M_\odot = 1.99 \times 10^{30}$ kg) and a radius of 100 km, and that it collapses to a uniform sphere of neutrons of radius 10 km. Assume that the virial theorem

$$2\langle T\rangle + \langle V\rangle = 0$$

holds, where $\langle T\rangle$ is the average of the internal kinetic energy and $\langle V\rangle$ is the average of the gravitational potential energy. $E = \langle T\rangle + \langle V\rangle$ is the total mechanical energy of the system. Calculate the energy consumed in neutronization and the number of electron neutrinos produced. Given that the remaining energy is radiated as neutrino-antineutrino pairs of all kinds of average energy 12 + 12 MeV, calculate the total number of neutrinos radiated.

3. About 3 s after the onset of the Big Bang, the neutron-proton ratio became frozen when the temperature was still as high as 10^{10} K ($kT \simeq 0.8$ MeV). About 250 s later, fusion reactions took place converting neutrons and protons into ^{4}He nuclei. Show that the resulting ratio of the masses of hydrogen and helium in the universe was close to 3. The neutron half-life = 10.24 min and the neutron-proton mass difference is 1.29 MeV.

4. Given that the supernova of exercise 2 is at a distance of 163,000 light years, calculate the total number of neutrinos of all types arriving at each square meter of the earth. Also

estimate the number of reactions

$$\bar{\nu}_e + \mathrm{p} \longrightarrow \mathrm{n} + e^+$$

that will occur in 1000 metric tons of water. Assume that the cross section is given by

$$\sigma = \frac{4 p_e E_e G_F^2}{\pi \hbar^4 c^4}$$

where p_e and E_e are the positron momentum and energy, respectively, and G_F is the Fermi coupling constant. Assume that only one-sixth of the neutrinos are electron neutrinos.

5. Evaluate the radius of a neutron star with mass of 1.2 $M_\odot$.

6. The rate of energy delivered by the sun to the earth is known as the solar constant and equals 1.4×10^6 erg cm^{-2} s^{-1}. Knowing that the distance between the sun and the earth is of the order of 1.5×10^8 km, give a lower estimate of the rate at which the sun is losing mass to supply the radiated energy.

7. Calculate the energy radiated during the contraction of the primordial gas into the sun (the sun's diameter is 1.4×10^6 km). What energy would be released if the solar diameter were suddenly to shrink by 10%?

8. Given that the sun was originally composed of 71% hydrogen by weight and assuming it has generated energy at its present rate (3.86×10^{36} W) for about 5×10^9 years by converting hydrogen into helium, estimate the time it will take to burn 10% of its remaining hydrogen. Take the energy release per helium nucleus created to be 26 MeV.

9. The CNO cycle that may contribute to energy production in stars similar to the sun begins with the reaction $\mathrm{p} + {}^{12}C \rightarrow {}^{13}N + \gamma$. Assuming the temperature near the center of the sun to be 15×10^6 K, find the peak energy and width of the reaction rate.

10. Assume that we know the bound state wavefunction for the relative motion of particles *a* and *b*. Initially, the particles are thought to be in a quasi-stationary excited state of the compound nucleus. There is an exponential decrease of the wavefunction through the potential barrier which turns into an outgoing wave at infinity. We define the decay rate of that state (for particle emission) as

$$\lambda = \frac{1}{\tau} = \text{probability/sec for a decay through a large spherical shell.}$$

(a) If the wavefunction is written as

$$\Psi_{nlm} = \frac{u_l(r)}{r} Y_{lm}(\theta, \phi),$$

show that $\lambda = \nu \left| u_l(\infty) \right|^2$.

We define the penetration factor for particles of relative angular momentum l as

$$P_l = \frac{|u_l(\infty)|^2}{|u_l(R)|^2},$$

where $r = R$ is a position where the nuclear potential is close to zero (see figure 12.17 below).

Thus the decay rate can be written as $\lambda = \nu P_l |u_l(R)|^2$. For a uniform probability density inside the compound nucleus

$$|u_l(R)|^2 dr = \frac{4\pi R^2 dr}{4\pi R^3/3} = \frac{3}{R} dr .$$

One defines the reduced width θ_l by means of

$$|u_l(R)|^2 = \theta_l^2 \frac{3}{R}.$$

For realistic nuclear states

$$0.01 < \theta_l^2 < 1,$$

and θ_l^2 gives a measure of the degree to which a quasi-stationary nuclear state can be described by a relative motion of a an b in a potential.

(b) Show that the partial width of that state is given by

$$\Gamma_l = \frac{3\hbar\nu}{R} P_l \theta_l^2.$$

(c) Show that for charged particles, with

$$V_l(r) = \begin{cases} l(l+1)\hbar^2/2\mu r^2 + Z_1 Z_2 e^2/r & (r > R), \\ l(l+1)\hbar^2/2\mu r^2 + V_N & (r < R), \end{cases}$$

we get

$$P_l = \frac{1}{F_l^2(R) + G_l^2(R)},$$

where F_l and G_l are the regular and irregular Coulomb functions.

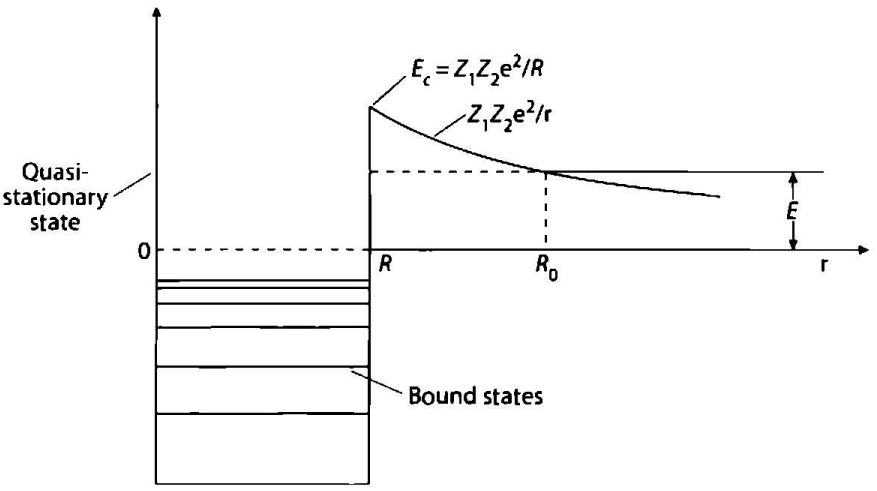

Figure 12.17 Potential barrier for charged particles.

(d) Show that using WKB wavefunctions for $u_l(r)$, one gets

$$P_l = \left[\frac{V_l(R) - E}{E}\right]^{1/2} \exp\left\{-\frac{2\sqrt{2\mu}}{\hbar}\int_R^{R_0}\left[V_l(r) - E\right]^{1/2} dr\right\}. \tag{12.100}$$

with $l(l+1) \to (l+1/2)^2$.

11. A numerical computation of the above equation shows that a good approximation consists in replacing $V_l(R) - E \cong E_c = Z_1 Z_2 e^2/R$ in the factor preceding the exponential. This approximation is justified since at astrophysical energies $E \ll E_c$.

(a) Calling the exponent in (12.100) W_l, show that, to lowest order in E/E_c,

$$W_0 = 2\pi \frac{Z_1 Z_2 e^2}{\hbar v}\left[1 - \frac{4}{\pi}\left(\frac{E}{E_c}\right)^{1/2} + \frac{2}{3\pi}\left(\frac{E}{E_c}\right)^{3/2} - \cdots\right]. \tag{12.101}$$

(b) Write the expression for the lifetime, Γ_0, of a state with $l = 0$ in terms of the reduced width θ_0^2 (see exercise 10) and W_0. Show that, to first order in E/E_c,

$$\Gamma_0 \propto \exp\left(-bE^{-1/2}\right).$$

12. For $l \neq 0$,

$$W_l = \frac{2\sqrt{2\mu}}{\hbar}\int_R^{R_0}\left[E_c\frac{R}{r} + E_l\left(\frac{R}{r}\right)^2 - E\right]^{1/2} dr\,.$$

where $E_l = \left(l + \frac{1}{2}\right)^2 \hbar^2/2\mu R^2$. For astrophysically relevant cases, $R/R_0 \lesssim 10^{-3}$ and the ratio R/r is quite small for most range of the integration. As a consequence the second term in the square root bracket never dominates, and the integrand may be expanded, whereupon the leading terms become

$$W_l \simeq \frac{2\sqrt{2\mu}}{\hbar}\int_R^{R_0}\left(E_c\frac{R}{r} - E\right)^{1/2} dr + \frac{\sqrt{2\mu}}{\hbar}\int_R^{R_0}\frac{E_l R^{3/2}}{E_c^{1/2}}\frac{dr}{r^{3/2}}. \tag{12.102}$$

The first term is just equal to W_0, whereas the second term reflects the additional effects of the centrifugal barrier.

(a) Show that (12.102) becomes

$$W_l = W_0 + 2\left[\frac{(l+1/2)^2 E_l}{E_c}\right]^{1/2}\left[1 - \left(\frac{E}{E_c}\right)^{1/2}\right].$$

(b) Neglecting the correction in $(E/E_c)^{1/2}$ in the above equation, show that

$$P_l \approx \left(\frac{E_c}{E}\right)^{1/2} \exp\left[-2\pi\frac{Z_1 Z_2 e^2}{\hbar v} + 4\left(\frac{2\mu R^2 E_c}{\hbar^2}\right)^{1/2} - 2(l+1/2)^2\left(\frac{\hbar^2}{2\mu R^2 E_c}\right)^{1/2}\right],$$

where the correction of order (E/Ec)^3/2 has also been dropped.

(c) Show that

$$\Gamma_l = 6\theta_l^2 \left(\frac{\hbar^2 E_r}{2\mu R^2}\right)^{1/2} \exp(-W_l). \tag{12.103}$$

(d) The reaction $^{12}C(p,\gamma)^{13}N$ has a peak at 424 keV center of mass energy, corresponding to a $J^\pi = \frac{1}{2}^+$ resonance. The resonance has a full width at half maximum $\Gamma = 40$ keV. This width is essentially the proton width, since the only other channel is Γ_γ, which is much smaller than Γ_p. What is the value of the dimensionless reduced width θ_l^2 for that state?

13. (a) Show that close to a resonance the astrophysical S-factor is given by

$$S(E) = \frac{\pi\hbar^2}{2\mu} \frac{g\Gamma_\alpha(E)\Gamma_\beta(E)}{(E-E_r)^2 + \Gamma^2/4} \exp\left(2\pi \frac{Z_1 Z_2 e^2}{\hbar v}\right).$$

where $g = (2J+1)/(2J_\alpha + 1)(2J_\beta + 1)$ is the statistical spin factor. The decay widths for the entrance and decay channels, $\Gamma_\alpha(E)$ and $\Gamma_\beta(E)$, respectively, also depend on the energy for reactions of astrophysical interest.

(b) In some situations, Γ_β is approximately constant, that is, when the final channel is a γ- or α- decay. In this case, use (12.103) for $\Gamma_\alpha^{(l)}(E)$ and write an expression for $S(E)$ in terms of $l, E, E_c, \Gamma_\beta^{(l)}$, and Γ.

14. In stellar interiors, and also in laboratory experiments, the nuclear fusion cross sections for naked nuclei are modified due to the presence of electrons. The electron shielding around the nuclei is equivalent to a constant (negative) potential U_e that is usually much smaller than the energy E.

(a) Show that this potential modifies the fusion cross section so that

$$\sigma_{\text{screened}}(E) = \exp\left(\pi\eta \frac{U_e}{E}\right) \sigma_{\text{bare}}(E).$$

Find in the literature the experimental values of U_e (screening by electrons in the target) for five reactions of astrophysical interest. Comment about the comparison with theoretical values.

15. Show that for a resonant (p,γ) cross section reaction, for example, $^{12}C(p,\gamma)^{13}N$ at 424 keV, one finds

$$\langle\sigma v\rangle_{\text{resonant}} = \left(\frac{2\pi}{\mu kT}\right)^{3/2} \frac{\Gamma_p\Gamma_\gamma}{\Gamma} e^{-E_r/kT}.$$

16. The nonexistence of a bound nucleus with $A = 8$ was one of the major puzzles in nuclear astrophysics. How could heavier elements than $A = 8$ be formed? Using typical values of concentration of α-particles in the core of a heavy star, $n_\alpha \sim 1.5 \cdot 10^{28}/\text{cm}^3$ (corresponding

to $\rho_\alpha \sim 10^5$ g/cm^3) and $T_8 \sim 1$, one obtains

$$\frac{n(^8\text{Be})}{n(\alpha)} \sim 3.2 \times 10^{-10}.$$

Salpeter suggested that this concentration would then allow $\alpha + {}^8\text{Be}(\alpha+\alpha) \rightarrow {}^{12}\text{C}$ to take place. Hoyle then argued that this reaction would not be fast enough to produce significant burning unless it was also resonant. Now the mass of ${}^8\text{Be} + \alpha$ is 7.366 MeV, and each nucleus has $J^\pi = 0^+$. Thus s wave capture would require a 0^+ resonance in ${}^{12}\text{C}$ at ~ 7.4 MeV. No such state was then known, but an experimental search revealed a 0^+ level at 7.644 MeV, with decay channels ${}^8\text{Be} + \alpha$ and γ-decay to the 2^+ 4.433 level in ${}^{12}\text{C}$. The parameters are

$\Gamma_\alpha \sim 8.9\text{eV},$

$\Gamma_\gamma \sim 3.6 \cdot 10^{-3}\text{eV}.$

(a) Show that

$$r_{48} = n_\alpha^3 \, T_8^{-3} \exp\left(-\frac{42.9}{T_8}\right) (6.3 \cdot 10^{-54}\text{cm}^6/\text{sec}).$$

If we denote by $\omega_{3\alpha}$ the decay rate of an α in the plasma, then

$$\omega_{3\alpha} = 3\, n_\alpha^2 \, T_8^{-3} \exp\left(-\frac{42.9}{T_8}\right) (6.3 \cdot 10^{-54}\text{cm}^6/\text{sec})$$
$$= \left(\frac{n_\alpha}{1.5 \cdot 10^{28}/\text{cm}^3}\right)^2 (4.3 \cdot 10^3/\text{sec}) \, T_8^{-3} \exp\left(-\frac{42.9}{T_8}\right).$$

(b) Since the energy release per reaction is 7.27 MeV show that the energy produced per gram, ϵ, is

$$\epsilon = (2.5 \cdot 10^{21}\text{erg/g sec}) \left(\frac{n_\alpha}{1.5 \cdot 10^{28}/\text{cm}^3}\right)^2 T_8^{-3} \exp\left(-\frac{42.9}{T_8}\right).$$